Published in final edited form as:
Prog Brain Res. 2012 ; 196: 235–263. doi:10.1016/B978-0-444-59426-6.00012-4.

Optogenetic Reporters: Fluorescent Protein-Based Genetically-Encoded Indicators of Signaling and Metabolism in the Brain

Mathew Tantama, **Yin Pun Hung**, and **Gary Yellen***
Department of Neurobiology, Harvard Medical School, 200 Longwood Avenue, Boston, Massachusetts, 02115

Abstract

Fluorescent protein technology has evolved to include genetically-encoded biosensors that can monitor levels of ions, metabolites, and enzyme activities as well as protein conformation and even membrane voltage. They are well suited to live-cell microscopy and quantitative analysis, and they can be used in multiple imaging modes, including one or two-photon fluorescence intensity or lifetime microscopy. Although not nearly complete, there now exists a substantial set of genetically-encoded reporters that can be used to monitor many aspects of neuronal and glial biology, and these biosensors can be used to visualize synaptic transmission and activity-dependent signaling *in vitro* and *in vivo*. In this review we present an overview of design strategies for engineering biosensors, including sensor designs using circularly-permuted fluorescent proteins and using fluorescence resonance energy transfer (FRET) between fluorescent proteins. We also provide examples of indicators that sense small ions (e.g., pH, chloride, zinc), metabolites (e.g., glutamate, glucose, ATP, cAMP, lipid metabolites), signaling pathways (e.g., G protein coupled receptors, Rho GTPases), enzyme activities (e.g., protein kinase A, caspases), and reactive species. We focus on examples where these genetically-encoded indicators have been applied to brain-related studies and used with live-cell fluorescence microscopy.

Keywords

Genetically-encoded; biosensor; fluorescent protein; circularly-permute; resonance energy transfer; FRET; live-cell microscopy

Introduction

Fluorescent proteins (FPs) have proven to be an incredibly versatile platform for engineering sensors of enzyme activities, membrane voltage, ions, molecules, and proteins (Frommer *et al.*, 2009; Knopfel *et al.*, 2010; Newman *et al.*, 2011). Since the first Ca^{2+} sensors were reported (Miyawaki *et al.*, 1997; Romoser *et al.*, 1997), the number and variety of FP-based sensors have grown immensely, and many extensive reviews on their design and application in cell biology have been written (Frommer *et al.*, 2009; Chudakov *et al.*, 2010; Newman *et al.*, 2011). In this chapter, we provide examples of FP-based sensors that have been applied specifically to brain-related studies. Advances in fluorescent protein engineering, calcium sensors, and voltage sensors are covered in other chapters of this volume, and therefore we do not focus on these topics. We first discuss major strategies for engineering genetically-targeted FP-based sensors, and then we provide several examples organized by sensor target.

CORRESPONDING AUTHOR: Gary Yellen, Ph.D., Professor of Neurobiology, gary_yellen@hms.harvard.edu, Tel: 617-432-0137, Fax: 617-432-0121.

Genetically-Encoded Indicators (GEIs)

Several design strategies have been used to engineer genetically-encoded sensors that provide a fluorescence readout for the level of an analyte (small molecule or ion) or the activity of a signaling system (Figure 1). We refer to this broad class of sensors as genetically-encoded indicators (GEIs), borrowing terminology from genetically-encoded calcium indicators (GECIs). A GEI has two functional units, the ***sensor domain*** and the ***reporter domain***. The reporter domain is a single FP or a pair of FPs that provides the fluorescence readout. The sensing domain can be a peptide motif, a full protein, or a combination of the two that senses the target of interest. In practice, the ***coupling*** between the sensor and reporter domains influences most of the GEI characteristics, including fluorescence spectra, type of response, and the dynamic range. We discuss different GEI design and sensing parameters in this section.

Once a target of interest has been identified, the choice and design of the sensor domain is the first consideration for GEI construction. In order to elicit a fluorescence response from the GEI, ligand binding or enzymatic modification must cause a change in molecular conformation. Although some artificial sensing scaffolds have been engineered, these often lack specificity for the intended target (Vinkenborg et al., 2010). Rather, a highly successful strategy relies on naturally-occurring sensor domains that can be adapted for GEI construction. For example, the Cameleon family of Ca^{2+} sensors exploits Ca^{2+}-dependent binding of calmodulin (CaM) and the M13 peptide (Miyawaki *et al.*, 1997; Romoser *et al.*, 1997). The physical change induced by Ca^{2+} is coupled to a perturbation of the reporting domain, that is, the Ca^{2+}·CaM-M13 binding energy is used to do work to alter the GEI fluorescence.

The choice of the color and the number of FPs for the reporter domain is the next design consideration. We consider reporter domains that consist of either one or two FPs. In single FP GEIs, the physical change in the sensor domain causes a chemical or structural change in the local environment of the FP chromophore, altering its intrinsic fluorescence characteristics. The sensitivity to this structural change can be natural, engineered through point mutations, or engineered by a circular permutation strategy. In dual FP GEIs, the physical change in the sensor domain causes a change in resonance energy transfer between the two FPs. We discuss each of these strategies in greater detail in later sections.

After choosing sensor and reporter domains, engineering the coupling between the domains is the most critical process of GEI development, and coupling must be optimized to obtain desirable GEI characteristics. Structure-guided design can significantly aid the rational development of GEIs (Wang *et al.*, 2008a; Akerboom *et al.*, 2009), but empirical discovery remains a substantial component of the process. For example, optimizing the length and composition of the peptide linkers connecting the sensor and reporter domains is often a critical process, but it is also a major hurdle that largely relies on random trial and error. The process of optimizing the coupling between domains can entail screening many libraries of mutants and iteratively improving the sensor's characteristics. In this development stage several parameters are considered, including the GEI's affinity for the target, the sensing range, the sensing kinetics, the type of fluorescence response, the dynamic range of the fluorescence response, the specificity of the response, and the perturbations expression of the sensor may cause.

The levels and dynamics of ions, metabolites, and enzymatic substrates are tightly regulated in biological systems, and thus the GEI's target affinity, sensing range, and sensing kinetics must be well-tuned to respond to physiological changes. The GEI's apparent affinity for its target (K_{app}) describes the point of half-maximal activation or saturation by a target ligand.

The sensing range describes the range of target concentrations or activities over which distinct signals can be detected. Both are described by the GEI's dose-response curve (Figure 2). The sensing range is dictated by the steepness of the dose-response. For example, a sensor domain with multiple ligand binding sites may exhibit large positive cooperativity and a steep response curve, resulting in a narrow sensing range. This type of sensing may be useful for a binary readout or an "on-off" sensor, but it is not ideal for monitoring graded responses. Related to the affinity, the sensing kinetics are determined by the on and off rates of the target, the rate of the conformational change of the sensor domain, and the rate of coupling between the sensor and reporter domains. Ideally, the K_{app} and sensing range will match the physiological midpoint and target level range, and the response time will be faster than the kinetics of endogenous signaling.

When optically monitoring GEIs, the fluorescence response can be either a simple intensity change or a ratiometric change that affects the relative intensity at different wavelengths. Intensity-based measurements use a single excitation wavelength and monitor fluorescence changes at a single emission wavelength. However, the fluorescence intensity also depends on the concentration of the fluorophore, and comparison of absolute intensity changes is usually not possible because of cell-to-cell and experiment-to-experiment variability in GEI expression levels. Instead, intensity measurements generally are used to monitor relative changes during an experimental manipulation. Ratiometric measurements eliminate the dependence on fluorophore concentration, enabling direct comparisons between experiments that facilitate quantitative analysis. Ratiometric measurements can either use two excitation wavelengths and monitor a single emission (excitation ratiometric) or use a single excitation and monitor two emission wavelengths (emission ratiometric). For example, an excitation ratiometric GEI exhibits two peaks in its basal fluorescence excitation spectrum. When the GEI senses its target, the excitation spectrum changes in a specific manner: one peak increases, the other peak decreases, and there exists a wavelength that shows no intensity change called the isosbestic point. The ratio of the peak intensities is the readout of the ratiometric GEI.

Regardless of whether it is an intensity or ratiometric change, the dynamic range of the fluorescence response must also be maximized to improve the signal-to-noise and detection of changes. The fluorescence dynamic range describes the maximal detectable change in the fluorescence response. Although the two are functionally related, the dynamic range of the fluorescence response and the sensing range are distinct parameters (Figure 2). It is important to note that the dynamic range of the fluorescence response may differ substantially between purified protein in solution and protein expressed intracellularly because of environmental factors.

In the process of optimizing the GEI's characteristics, it is critical to verify the specificity of the response to the target. The sensor domain may have substantial affinity for structurally related analytes or closely-related enzyme activities, or there may be naturally occurring allosteric modulators. Rational mutagenesis and screening in some cases can reduce off-target interference, especially if structure-function studies of the endogenous sensor domain are available to guide mutagenesis. At the very least, a reasonable effort should be made to identify interfering factors so that the proper experimental controls can be conducted when using the GEI. Interference can also result from environmental sensitivity of the FPs, for example to pH, as will be discussed in a later section.

Finally, care must be taken when using naturally-occurring sensing domains because they can interact with and alter endogenous processes, especially if the sensing domain has a natural enzymatic activity. To diminish interference by Cameleon, the CaM and M13 were mutated in parallel to maintain recognition for one another but abrogate recognition by

endogenous CaM (Palmer et al., 2006). Another approach is to choose a sensing domain from a species different from that under study. For example, bacterial periplasmic proteins have been exploited for sensing analytes in mammalian systems to reduce the possibility of biological cross-talk (Okumoto et al., 2008). A related concern is that the GEI itself can cause pathological buffering of the analyte, interfering with endogenous signaling by changing the free concentration. FPs and GEIs may reach micromolar concentrations when expressed in cells, and analytes whose intracellular concentration is near or less than this may be affected. Some analytes occur at low free concentrations but have a much higher total concentrations due to endogenous buffering, and these analytes may be less affected by sensor expression. However, pathological buffering by the GEI can be a large problem for analytes that occur at low total concentrations.

Clearly, engineering an optimal GEI with respect to all of these parameters is not trivial, but many useful GEIs have been developed that have provided important insight into brain function, despite deficiencies in one or more of their sensing properties. We next describe in greater detail design strategies based on single FP environmental sensitivity, circular permutation of a single FP, resonance energy transfer between two FPs, or translocation of FPs.

GEIs Using Environment Sensitive Fluorescent Proteins

Although the FP β-barrel structure substantially shields the interior chromophore from the environment, it is important to realize that FPs still can respond to external changes, and in particular all FPs exhibit some degree of pH sensitivity (Day and Davidson, 2009; Chudakov *et al.*, 2010). Environmentally sensitive intrinsic fluorescence can be a result of the acid-base chemistry of the chromophore (Bizzarri et al., 2009). Channels for solvent access or proton relay networks can couple the interior environment near the chromophore to changes in the external solution (Wachter *et al.*, 1998; Jayaraman *et al.*, 2000). It is well known that pH often changes with neuronal activity, metabolism, and intracellular signaling (Chesler and Kaila, 1992; Srivastava *et al.*, 2007; Bizzarri *et al.*, 2009; Casey *et al.*, 2010). This is a critical issue for GEIs because the fluorescence change due to a pH transient can be of the same magnitude as the maximum fluorescence response to its target, and thus the GEI fluorescence response can be aliased with pH transients. In this section we briefly describe how chromophore acid-base chemistry affects the intrinsic fluorescence of FPs. We also describe the related phenomenon of excited-state proton transfer. Finally, we discuss how natural or engineered environmental sensitivity can be exploited in GEIs.

The wild type green fluorescent protein (GFP) chromophore can exist in different ionization states, and the protonated neutral form has distinct photophysical properties from the deprotonated anionic form (Tsien, 1998; Bizzarri *et al.*, 2009). The GFP chromophore is a *p*-hydroxybenzylidene-5-imidazolidinone (*p*-HBI), containing a phenol group derived from Tyr66 that can be deprotonated to form an anionic chromophore (Figure 3). In solution, the pK_a of a phenol hydroxyl proton is ~10; however, the pK_a of the *p*-HBI phenol is lowered by the conjugated π-system of the chromophore and the protein environment, shifting the pK_a to a value of ~8 or less depending on the specific FP. In GFP, a bound water, Ser205, and Glu222 form a proton relay network that can accept a proton from the chromophore, and Thr203 can rotate to stabilize the phenolate anion. The protonated neutral state (“A” state) and the deprotonated anionic state (“B” state) are important to consider because protonation of the chromophore changes its absorbance and fluorescence properties. The A state of GFP has an absorbance peak at 395 nm with a fluorescence emission peak at 508 nm, but the B state has an absorbance peak at 475 nm with a fluorescence emission peak at 503 nm. Peak absorbance of the B state occurs at a longer wavelength because deprotonation of the chromophore decreases the transition energy between the ground and excited state. The

internal conformation of wild type GFP favors the A state, and there is only a minor population of the B state in neutral solution. In contrast, the S65T mutation of the enhanced GFP (EGFP) mutant favors the B state, and as a result EGFP peak excitation and fluorescence emission occur at 488 nm and 508 nm, respectively. Many engineered GFP variants show significant coupling between the external pH and chromophore protonation, with apparent pK_a values of 5 to 6.5 (Chudakov et al., 2010). Therefore, the chromophore may exist in an equilibrium of ionization states that is sensitive to changes in solution pH, resulting in pH-dependent fluorescence.

The protonated neutral state of wild type GFP has a large Stokes shift (the difference between the excitation and emission wavelengths) because of excited-state proton transfer (ESPT) (Tsien, 1998; Bizzarri *et al.*, 2009). Excitation at 395 nm generates an excited state of the protonated neutral chromophore (A*), and in this excited state the *p*-HBI phenol is more acidic. The phenol deprotonates through excited-state proton transfer to the aforementioned proton relay network, creating an excited-state anion (I*). The transition energy is decreased for relaxation from the I* anionic excited-state, and peak fluorescence emission after ESPT is red-shifted to 508 nm. In the absence of ESPT, relaxation from the A* protonated excited-state is a higher energy transition with peak fluorescence emission at 460 nm; however, ESPT is efficient and occurs on the time scale of ~10 ps in GFP, resulting in effectively a single emission peak at 508 nm. Of note, the I* excited-state anion is distinct from the B* excited-state anion. As previously mentioned, the B state is stabilized by conformational rearrangements including rotation of Thr203, and the A and B states represent not only distinct ionization states but also distinct internal protein conformations. After ESPT from A* to create the I* excited-state anion, fluorescence emission occurs before a conformational change can transpire. Thus, peak fluorescence emission from I* and B* excited-states are very similar but not exactly equal in energy.

For yellow fluorescent proteins (YFPs), chloride and pH sensitivity are interrelated (Jayaraman et al., 2000). In YFPs, Thr203 is mutated to an aromatic amino acid such as Tyr. The aromatic residue can π-stack with the chromophore, decreasing the energy gap between the anionic B and B* states. The mutation also creates an accessible halide binding site close to the chromophore. When a halide such as Cl^- binds, the additional negative charge stabilizes the protonated A state of the chromophore. Thus, Cl^- binding can shift the apparent pK_a of the YFP, making its fluorescence sensitive to changes in Cl^- concentration (Wachter *et al.*, 2000; Griesbeck *et al.*, 2001).

Sensitivity to pH and Cl^- can clearly affect the intrinsic fluorescence of FPs, but this can be exploited to create GEIs precisely for H^+ and Cl^-. This type of GEI uses only a single environmentally-sensitive FP that acts as both the sensor and reporter domains (Figure 1A). Mutagenesis can be used to tune its sensing characteristics, to alter the chromophore acid-base chemistry, or to alter the ESPT reaction to create excitation or emission ratiometric GEIs (Miesenbock *et al.*, 1998; Hanson *et al.*, 2002). Furthermore, mutagenesis can also introduce additional, non-natural environmental sensitivity. For example, by introducing cysteines in the exterior β-barrel near the chromophore, the roGFPs and rxYFPs were engineered to be sensitive to reduction and oxidation (Ostergaard *et al.*, 2001; Hanson *et al.*, 2004). We discuss specific examples of pH, Cl^-, and reduction-oxidation sensitive FPs of this type in the later sections. More commonly, the sensing domain is a distinct unit, and the remaining designs coopt natural peptides or proteins for this purpose.

GEIs Using Circularly Permuted Fluorescent Proteins

Circular permutation of a single FP is one strategy used to couple a conformational change in the sensor domain to a perturbation of the chromophore. The native FP termini are

spatially distant from the chromophore, and typically movements of the termini do not alter the chromophore or the intrinsic fluorescence. In a circularly-permuted FP (cpFP), the original N-and C-termini are ligated by a short peptide linker, and new termini are created (Baird et al., 1999). If the new termini are located spatially close to the chromophore, physical movements of the termini may alter the local environment around the chromophore. The altered cpFP conformation often increases solvent accessibility to the chromophore or shifts the acid-base equilibrium, causing a change in the intrinsic fluorescence.

For example, in the calcium sensor GCaMP Ca^{2+}-dependent binding between calmodulin (CaM) and the M13 peptide alters the fluorescence intensity of cpEGFP (Nakai et al., 2001). In this sensor EGFP is circularly permuted at residue 149, and the new termini are attached to CaM and the M13 peptide (Figure 1B). In the absence of Ca^{2+}, apo-GCaMP2 has a peak absorbance at 399 nm characteristic of the GFP protonated A state; however, it has very low fluorescence, suggesting that non-radiative decay is favorable. Bound to Ca^{2+}, the peak absorbance shifts to 488 nm, and a conformational change in the CaM-M13 binding pair stabilizes a fluorescent deprotonated B state (Wang *et al.*, 2008a; Akerboom *et al.*, 2009). Circular permutation was exploited here to couple a conformational change in the sensor domain to a shift in the cpEGFP acid-base equilibrium, creating a GEI that responds with simple fluorescence intensity changes.

Circular permutation also can be used to create GEIs that respond with a ratiometric fluorescence change, and the cpEYFP-based Ca^{2+}-sensor Pericam is one example (Nagai et al., 2001). Ratiometric Pericam exhibits Ca^{2+}-dependent changes in its absorbance spectrum similar to GCaMP2, but excitation of the A state produces fluorescence emission. Mutagenesis of cpEYFP at His148 and Thr203 created a variant in which non-radiative decay after excitation of the A state is decreased and in which ESPT is efficient. Excitation of both the protonated A (418 nm) and deprotonated B (494 nm) states produces a peak fluorescence emission at 511 nm. Thus, binding of Ca^{2+} produces a shift in the fluorescence excitation spectrum of Ratiometric Pericam.

While circular permutation is a versatile and important design strategy for engineering GEIs, one major disadvantage of using cpFPs is that circular permutation can increase pH sensitivity. Analyte binding to a cpFP-based GEI typically affects the protonation of the chromophore, producing a shift in the A and B state populations. When measured at constant pH, the fluorescence response reflects analyte concentration; but when measured as a function of pH, the binding of analyte is seen simply to shift the pK_a. This means that a simple change in pH can mimic the effect of a change in analyte concentration when in fact there is none. Artifacts due to pH changes can plague both intensity and ratiometric cpFP-based GEIs (Nagai et al., 2001). Proper use of these sensors thus requires either very tight control of pH or simultaneous measurement of pH using an additional sensor (see the section below on pH sensors).

GEIs Using Förster Resonance Energy Transfer

Förster-type resonance energy transfer (FRET) between two FPs is another strategy used to couple a conformational change in the sensor domain to a fluorescence response. Unlike the circular permutation strategy, FRET-based sensing does not involve a structural or chemical change in the chromophore of either FP. Instead, the efficiency of energy transfer between the two chromophores is altered by a conformational change in the sensor domain. After light absorption, an excited-state fluorophore typically relaxes back to the ground state by fluorescence emission or by a non-radiative decay mechanism (such as collision with a solvent molecule). When an excited-state donor fluorophore is in close proximity to an acceptor chromophore, the donor can additionally relax by transferring energy to the

acceptor via a dipole-dipole interaction, if the donor's emission spectrum overlaps with the acceptor's absorbance spectrum. When the acceptor itself is a fluorophore, the FRET-induced acceptor excited state can subsequently relax by acceptor fluorescence emission. Note that the acceptor chromophore does not itself need to be fluorescent, and FRET sensors with dark acceptors are useful for fluorescence lifetime applications (Murakoshi et al., 2008). The efficiency of FRET is very sensitive to the distance and the relative orientation between the donor and acceptor. GEIs can exploit FRET by attaching compatible FPs (a FRET pair) to different sensor domains that interact (intermolecular FRET) or by attaching the FRET pair to a single sensor domain (intramolecular FRET).

Intermolecular FRET has been used to detect protein-protein interactions because of its strong distance dependence. A key parameter is the Förster radius, R_0, which is the distance between the acceptor and donor at which the FRET efficiency is 50%. For FP pairs, R_0 is approximately 4 – 5 nm (Patterson et al., 2000). When two proteins are tagged each with one FP of a FRET pair, substantial FRET suggests close proximity and a potential interaction between the proteins. It is generally assumed that a decrease in FRET indicates dissociation of the proteins. Interpretation of a FRET decrease must be treated with care, however, because FRET is so sensitive to the distance and relative orientation between the FRET pair. That is, a conformational change could also decrease FRET efficiency without disrupting a stable protein-protein interaction. For example, interpretation of FRET data has led to some controversy over G protein coupled receptor signaling and is discussed in a later section (Ciruela et al., 2010).

In GEIs that use intramolecular FRET, a conformational change in the sensor domain changes the efficiency of energy transfer between an attached FRET pair. For example, Cameleon is a FRET-based calcium sensor that exploits Ca^{2+}-dependent CaM-M13 binding (Miyawaki *et al.*, 1997; Romoser *et al.*, 1997). The sensor domain consists of CaM and the M13 peptide expressed as a fusion that is flanked on its ends by the FRET pair of enhanced blue FP (EBFP) and EGFP (Figure 1C). In the absence of Ca^{2+}, the sensor domain is extended, but when Ca^{2+} binds to Cameleon, Ca^{2+}·CaM binds the M13 peptide. This conformational change brings the EBFP and EGFP closer together, and the FRET efficiency increases. For intramolecular FRET-based GEIs, the FRET efficiency can be measured by exciting the donor and comparing the donor and acceptor fluorescence emission intensities. Therefore, intramolecular FRET sensors are also ratiometric sensors.

Compared to cpFP-based GEIs, FRET sensors can show better pH insensitivity if the right FRET pair is chosen. There are several FPs that have low pK_a values and whose fluorescence is pH insensitive in the physiological pH range (Chudakov et al., 2010). However, it is still important to clearly test pH sensitivity of the final construct because the sensor domain also can confer pH sensitivity to the GEI.

One disadvantage of intramolecular FRET-based GEIs is that there is a tendency for the fluorescence response to change only subtly. For intramolecular FRET sensors, there can be substantial basal FRET because the physical linkage of the FPs requires that they stay within a certain proximity to one another. Additionally, the size of the FPs limits the maximum absolute FRET efficiency. The FP β-barrel is ~4 nm in height and ~2.5 nm in diameter (Tsien, 1998; Day and Davidson, 2009), and the Förster radius for FP pairs is typically 4 – 5 nm. Therefore, the axial diameter of the β-barrel limits the closest possible distance between the acceptor and donor chromophores. It has been estimated that the maximum absolute FRET efficiency for FP pairs is ~50% (Patterson et al., 2000). Interestingly, cpFPs have been used to improve the dynamic range of the FRET response (Nagai et al., 2004). Here, unlike cpFPs discussed previously, circular permutation is used to alter the apparent relative

orientation of the FRET pair and not to induce an environmentally responsive chromophore (Baird et al., 1999).

GEIs Using Translocation Responses

Changes in the spatial distribution of FP-labeled proteins also can be used as a readout of analyte concentration or protein activity (Figure 1D). Translocation GEIs have been used extensively to monitor activation of G-protein coupled receptors and downstream signaling related lipid metabolism (Ciruela *et al.*, 2010; Newman *et al.*, 2011). For example, EGFP can be fused to a pleckstrin homology (PH) domain that binds phosphatidylinositol-(4,5)-bisphosphate (PIP_2) in the plasma membrane and also binds inositol-(1,4,5)-trisphosphate (IP_3) in the cytosol. When membrane PIP_2 concentration is high and cytosolic IP_3 concentration is low, PH-EGFP enriches in the plasma membrane. When a phospholipase is activated, PIP_2 is hydrolyzed to IP_3 and diacylglycerol, and PH-EGFP translocates to the cytosol. Thus, changes in the spatial distribution of PH-EGFP indicates changes in PIP_2 and IP_3 levels or activity of a phospholipase. The use of translocation GEIs requires microscopy with sufficient spatial resolution.

In the next sections, we provide examples in which GEIs have been used in brain-related studies. The sections are organized by the target analyte or protein activity being monitored. When available, we focus on examples of live-cell imaging of GEIs.

pH

Although several pH-sensitive FPs have been developed (Bizzarri et al., 2009), the pHluorin pH-sensors have been predominantly used to monitor synaptic transmission (Miesenbock et al., 1998). The pHluorins are single GFPs that contain mutations conferring significant pH sensitivity to their fluorescence, and they were engineered using structure-guided design (Miesenbock et al., 1998). Ratiometric pHluorin exhibits two peaks in its fluorescence excitation spectrum that respond ratiometrically to pH. Ecliptic pHluorin is an intensity-based GEI that is dark at pH < 6 and becomes fluorescent upon alkalinization. Ecliptic pHluorin was engineered to decrease background fluorescence, favoring a drastic intensity change and sacrificing a ratiometric response. The folding and fluorescence properties of ecliptic pHluorin were improved with two additional mutations, producing the now extensively used variant, superecliptic pHluorin (SEP) (Sankaranarayanan et al., 2000). At chemical synapses, neurotransmitters are loaded into acidic secretory vesicles. When a vesicle fuses with the plasma membrane to release its cargo, the vesicle lumen equilibrates with the extracellular environment causing a sharp alkalinization. When SEP is targeted to the lumen of synaptic vesicles, its fluorescence reports this pH transition, and hence SEP can be used to visualize synaptic vesicle cycling and synaptic transmission.

Superecliptic pHluorin has been targeted to the lumen of synaptic vesicles by fusing it to vesicle proteins such as VAMP2 (named synaptopHluorin or spH) (Sankaranarayanan and Ryan, 2001) or synaptophysin (named sypHy) (Granseth et al., 2006). New insights into the recycling modes of distinct presynaptic vesicle pools have been gained using these GEIs, but disputes over the kiss-and-run versus full-fusion mechanisms persist, often due to controversy over the methodology (Gandhi and Stevens, 2003; Fernandez-Alfonso and Ryan, 2004; Granseth *et al.*, 2006; Zhang *et al.*, 2009). Presynaptic vesicle cycling has been visualized using FM styryl dyes, pHluorin, and recently quantum dots, each with advantages and disadvantages. pHluorin overcame many problems associated the FM styryl dyes. The FM dyes require complicated loading protocols, they can lack specificity, and they can result in complicated response kinetics that confound interpretation (Ryan, 2001). Unlike FM dyes, pHluorin can be used to discriminate between the kinetics of endocytosis and exocytosis using an alkaline trapping method (Sankaranarayanan and Ryan, 2001). Quantum

dots have improved signal over noise compared to both FM dyes and pHluorin; however, quantum dots, like FM dyes, still require loading with stimulation protocols and are not easily loaded deep into tissue. pHluorins on the other hand have the powerful advantage of being amenable to genetic targeting and in vivo monitoring (Li et al., 2005).

Despite the controversy surrounding synaptic vesicle cycling, pHluorin fusions have been broadly used to monitor both pre- and postsynaptic function during synaptic transmission. Vesicle-targeted pHluorins provide an optical assay for investigating regulators of synaptic transmission, including small molecules (Thorsen et al., 2010) like isoflurane (Hemmings et al., 2005) and specific proteins. For example, a VGLUT1-pHluorin fusion was used to demonstrate that increased α-synuclein inhibits neurotransmitter release and decreases the size of the presynaptic vesicle pool that recycles (Nemani et al., 2010). On the postsynaptic side, a GluR1-pHluorin fusion was used to demonstrate that the AAA-ATPase Thorase is important for AMPA receptor endocytosis following NMDA stimulation, and Thorase may inhibit recycling of glutamate receptors by receptor disassembly (Zhang et al., 2011). In these examples, visualization of pHluorin was used in conjunction with genetic models to assess synaptic protein function with resolution of single neurons and synapses.

Populations of cells have also been imaged with pHluorin to study olfactory circuits and plasticity in live transgenic *Drosophila* and mice (Yu *et al.*, 2004; McGann *et al.*, 2005; Shang *et al.*, 2007). When pHluorin was genetically-targeted to the olfactory bulbs in mice or antennal lobes in flies, fluorescence changes correlated with population activity even though single synapses could not be visualized. The fluorescence readout provided a non-invasive optical method to investigate odorant coding. The use of pHluorin in this manner is powerful because it provides a means to monitor the activity of an intact network in a live animal.

In addition to synaptic transmission, many cellular processes involved with neuronal activity cause or rely on pH changes (Chesler and Kaila, 1992; Casey *et al.*, 2010). pHluorin has had a significant impact in brain research, but its primary use has not been to measure pH, perhaps overshadowing other GEIs of pH. Recently, the pH sensor mitoSypHer was used in astrocytes, and a decrease in mitochondrial pH was observed upon glutamate stimulation (Azarias et al., 2011). This GEI was engineered by modifying the hydrogen peroxide sensor HyPer (see section on Reactive Oxygen Species). HyPer contains a pH-sensitive YFP, and removing peroxide sensitivity created a ratiometric pH sensor (Poburko et al., 2011). Both cytoplasmic pH and mitochondrial matrix pH could be simultaneously monitored using the small molecule pH indicator SNARF-1 and mitoSypHer in the same cell.

Chloride

Chloride is a critical ion that influences membrane potential, cell volume, and pH. The FRET-based GEI for Cl^- called Clomeleon was first developed to measure intracellular chloride in hippocampal neurons and monitor GABAergic signaling (Kuner and Augustine, 2000). It is a tandem construct consisting of a cyan FP (CFP) and a chloride-sensitive YFP (Topaz), resulting in chloride-sensitive FRET. Clomeleon has several known performance issues: it has a low affinity (K_{app} ~ 90 mM) compared to the intracellular Cl^- concentration (~10 mM); Topaz is pH sensitive; and CFP and Topaz photobleach at different rates causing the FRET signal to change during strong or repeated illumination.

Despite these problems, Clomeleon has been useful for visualizing Cl^- in both cultured neurons and in brain slices from transgenic mice. For example, developmental changes in neuronal chloride concentration as well as transient GABA-evoked changes in intracellular chloride have been imaged with Clomeleon (Berglund *et al.*, 2006; Berglund *et al.*, 2008). In particular, Clomeleon was used to provide direct evidence for spatial Cl^- gradients in retinal

bipolar ON cells (Duebel et al., 2006). Perforated patch recordings had previously suggested that a Cl^- gradient existed, but the electrophysiology only provided indirect evidence. Using two-photon imaging of retinal preparations, an increased Cl^- concentration in dendrites compared to the soma was observed. The spatial gradient imaged with Clomeleon correlated with the functional consequence that GABA stimulation caused Cl^- influx at the soma but efflux at the dendrite.

Several studies using Clomeleon exemplify how GEIs and two-photon microscopy can be a very effective combination for imaging thick samples or deep in tissues. Preparations of brain slices or intact tissues are desirable because, compared to dissociated cultures, they better maintain physiologically relevant cellular environments, network connections, and anatomical relationships. Unfortunately, single-cell electrophysiology in thick preparations can be technically challenging and limit the number of cells that can be interrogated. Loading small-molecule indicators deep within tissues can also be inefficient. In contrast, GEIs such as Clomeleon can be genetically targeted, overcoming loading issues, and two-photon microscopy facilitates optically monitoring deep in tissues with the potential to interrogate several cells simultaneously. For example, imaging cerebellar slices from Clomeleon transgenic mice was used to visualize tonic inhibition of cerebellar granule cells by glial GABA release (Lee et al., 2010). Whole hippocampi and hippocampal slices from Clomeleon transgenic mice also have been used to observe pathological chloride accumulation in response to ischemia and epileptiform activity (Pond *et al.*, 2006; Glykys *et al.*, 2009; Dzhala *et al.*, 2010).

Clomeleon has been used most often for Cl^- visualization, but it is not the only GEI for Cl^-. An improved Clomeleon called Cl-sensor has been created using a similar FRET strategy. In Cl-sensor, Topaz has been replaced by a mutated YFP that increases the chloride affinity (K_{app} ~ 30 mM) and decreases the pH sensitivity (Markova et al., 2008). Intracellular chloride dynamics have been imaged in cultured neurons and retinal slices using Cl-sensor (Waseem et al., 2010). Additionally, a fusion of Cl-Sensor with the glycine receptor GlyR has been used to monitor chloride conduction and ion channel activity (Mukhtarov et al., 2008). Finally, transgenic mice that express a chloride-sensitive EYFP under control of the $K_V3.1$ promoter have also been generated (Metzger et al., 2002). Glutamate-evoked increases in Cl^- were imaged using hippocampal neuron cultures from these transgenic mice (Slemmer et al., 2004).

Zinc

Zn^{2+} is another biologically important ion that has been proposed to play a role in normal and pathological brain processes such as synaptic plasticity and excitotoxicity. Zn^{2+} has been found in glutamate containing synaptic vesicles in the cerebral cortex, it accumulates in neurons after excitotoxic injury, and it is an allosteric modulator of glutamate and GABA receptors (Frederickson et al., 2005). Chelation or exogenous application of Zn^{2+} can induce seizures and activate cell death programs. Physiological Zn^{2+} concentrations are tightly buffered, and free extracellular concentrations range from 1 to 10 nM while free intracellular concentrations may be in the nanomolar to picomolar range. Because it is highly buffered, Zn^{2+} is a challenging analyte to monitor (Vinkenborg et al., 2010).

A handful of both non-ratiometric intensity and ratiometric FRET GEIs of Zn^{2+} have been engineered (Vinkenborg et al., 2010). Zinc finger motifs containing His_4 and Cys_2His_2 binding sites have been used for sensor domains, but the GEIs using these binding motifs have affinities of ~ 2 – 200 μM, quite low compared to the expected free Zn^{2+} concentrations (Dittmer et al., 2009). Despite the low affinity, imaging the Cys_2His_2 sensor targeted to the mitochondrial matrix provided evidence that there is a high resting Zn^{2+}

concentration in the mitochondria of cultured hippocampal neurons. Furthermore, simultaneous imaging of mitochondrial Cys_2His_2-based sensor and the small molecule Zn^{2+} indicator FluoZin3 revealed that the neuronal response to glutamate depends on extracellular Zn^{2+}. In the absence of extracellular Zn^{2+}, glutamate stimulation causes mitochondrial Zn^{2+} release, but in the presence of extracellular Zn^{2+}, glutamate stimulation causes uptake and mitochondrial accumulation of Zn^{2+}. Improved GEIs with sub-nanomolar affinity for Zn^{2+} have been engineered, and these sensors should prove useful for future imaging of Zn^{2+} neurobiology (Vinkenborg *et al.*, 2010; Qin *et al.*, 2011).

Glutamate

Glutamate is the major excitatory neurotransmitter, and the dynamics of glutamate release and clearance affect synapse and network level signaling as well as neuron-glia metabolic coupling. Two similar FRET-based GEIs, FLIPE (Deuschle et al., 2005) and SuperGluSnFr (Hires et al., 2008), have been constructed using the same bacterial periplasmic binding protein ybeJ/GltI. This bacterial protein undergoes a hinge-like motion when glutamate binds to it. When ECFP and EYFP are fused to the termini of ybeJ/GltI so that they flank the binding protein, the glutamate-induced conformational change results in a change in FRET efficiency.

FLIPE and SuperGluSnFr have been used to visualize glutamate release in response to electrical stimulation and potassium chloride depolarization. Extracellular glutamate was monitored by expressing these GEIs on the surface of cultured hippocampal neurons (Okumoto *et al.*, 2005; Hires *et al.*, 2008). The imaging data suggested that reuptake by glial glutamate transporters mediates fast clearance following release, but at least in culture, significant spillover of several hundred nanomolar glutamate can still persist. Previous methods lacked the spatial and temporal resolution to perform this type of measurement.

These GEIs may prove valuable for evaluating glutamatergic synaptic transmission *in vivo*, but as of yet no genetic model or transient expression model has been published. There are published examples in which purified sensor was applied directly onto brain slices (Dulla et al., 2008). Despite the low resolution of these experiments, fluorescence transients that were imaged during stimulated activity correlated with electrical field potential recordings (Dulla et al., 2008). This method was used with an acute epileptiform brain slice model to show correlations among the inter-stimulus interval, the magnitude of the integrated field potential, and the size of the area for which GEI fluorescence reported glutamate release (Tani et al., 2010).

Glucose

Glucose is the primary energy source for the brain, and glucose-dependent metabolic rate is the basis for technologies such as FDG-PET scanning. Glucose metabolism classically has been observed through biochemical techniques that lack single-cell resolution such as isotope tracing or microdialysis. An engineered glucose-sensitive GEI provides much greater resolution of single-cell metabolism (Fehr et al., 2003). Like the GEIs for glutamate, the glucose sensor is one of a series of other stereotyped sensors based on bacterial periplasmic binding proteins used as the sensor domains (Okumoto et al., 2008). The bacterial MglB protein is flanked by ECFP and the YFP Citrine, and a glucose-induced conformational change alters the FRET efficiency. This glucose sensor has been significantly optimized (Takanaga et al., 2008), and a recent version $FLII^{12}Pglu\text{-}600\mu\delta6$ (also called $FLII^{12}Pglu\text{-}700\mu\delta6$) has been used to measure glucose metabolism in many cell types including cultured astrocytes and neurons (Bittner et al., 2010).

Direct measurements of glucose transport and metabolism have begun to emerge using this optimized glucose sensor. Independent measurements suggest that cultured astrocytes maintain their intracellular glucose concentration at half of the extracellular concentration in the steady-state. Upon inhibition of glucose transport, intracellular glucose rapidly decreases, indicative of hexokinase activity (Bittner et al., 2010). Interestingly, depolarization with potassium causes a rapid decline in intracellular glucose within seconds, and there is a rapid reversal upon removal of excess potassium (Bittner et al., 2011). In contrast, glutamate does not cause an acute decrease in intracellular glucose (Bittner *et al.*, 2011; Prebil *et al.*, 2011a; Prebil *et al.*, 2011b), but it does cause a slow increase in glucose concentration and glycolytic rate after several minutes (Bittner et al., 2011). Noradrenaline stimulation causes a rapid increase in intracellular glucose which can be partially attenuated by inhibition of glycogen phosphorylase (Prebil et al., 2011b). Future imaging of FLII^{12}Pglu-600μδ6 *in vivo* should help clarify many details of energy metabolism in neurons versus glia.

ATP

The dynamics of ATP production and hydrolysis in neurons and astrocytes is a critical aspect of brain energy metabolism and signaling. Recently, GEIs have been developed to visualize ATP. The sensor Perceval was engineered by inserting the circularly-permuted YFP cpVenus into the bacterial protein GlnK (Berg et al., 2009). When Mg·ATP binds to GlnK, there is protein loop movement at the binding site. By inserting the cpVenus into the loop region, the conformational change induced by Mg·ATP binding is coupled to a perturbation of the cpVenus chromophore. This perturbation causes a ratiometric shift in the Perceval's fluorescence excitation spectrum. The binding affinity for Mg·ATP is very high (K_{app} ~ 0.1 μM), and ADP can competitively bind to GlnK with lower affinity (K_{app} ~ 0.2 μM); however, ADP binding does not induce a loop movement. Furthermore, intracellular ADP and ATP concentrations are near 0.5 mM and 5 mM. As a result Perceval is always bound by either ADP or Mg·ATP, but the two nucleotides have distinct effects on the fluorescence. The combined result of these properties is that Perceval faithfully responds to changes in the ATP/ADP ratio independent of the total nucleotide level. The ATP/ADP ratio is indicative of the cellular energy status, and several ATP-dependent processes are sensitive to the ATP/ADP ratio. Perceval has proven useful for imaging energy depletion during metabolic inhibition of cultured cells.

Another GEI exploits the conformational change that occurs upon ATP binding to the ε subunit of the F_0F_1-ATP synthase (Imamura et al., 2009). By attaching the CFP mseCFP and cpVenus to the bacterial ε subunit, a series of GEIs called the ATeam sensors were engineered with varying affinities for ATP. These GEIs are insensitive to ADP and report absolute ATP concentrations. Similar to Perceval, ATeams were used to image ATP depletion during metabolic inhibition of cultured cells. Perceval and the ATeams are complementary GEIs, and in the future they should provide a great deal of information on neuronal and glial energy metabolism, especially if they are applied in conjunction with other GEIs such as the glucose sensor.

GPCR and Heterotrimeric G Protein Signaling

G protein coupled receptors (GPCRs) are critical components of the membrane-bound signal transduction machinery that affect synaptic transmission and plasticity. Ligand binding to the GPCR causes a conformational change to an active form. The activated GPCR acts as a guanine nucleotide exchange factor, activating heterotrimeric G-proteins ($G_{\alpha\beta\gamma}$) by promoting the replacement of bound GDP with GTP in the G_α protein. The activated G_α can subsequently activate downstream signaling before its intrinsic GTPase activity hydrolyzes

the bound GTP, causing auto-inactivation. Two major downstream pathways involve activation of phospholipase C (PLC) or activation/inhibition of adenylate cyclase. Activation of GPCRs has been monitored with several imaging probes (Lohse et al., 2008), including both intermolecular and intramolecular FRET-based GEIs. An important caveat of FP-based GEIs is that the bulky FP can interfere with protein-protein interactions, and the expressed GEI can interfere with endogenous signaling downstream of GPCR activation. Despite this caveat, FRET-based GEIs have been instrumental in delineating previously inaccessible GPCR and G-protein activation kinetics.

To monitor GPCR activation by intermolecular FRET, the separate components of the signaling complex, including the GPCR itself and the $G_{\alpha\beta\gamma}$ proteins, are fused to FRET compatible FPs such as CFP and YFP. GPCR activation causes a conformational change or dissociation of the GPCR, G_{α}, and $G_{\beta\gamma}$ proteins. When an appropriate pair of the signaling components is fused to FPs of a FRET pair, activation causes a decrease in FRET (Janetopoulos et al., 2001), but detailed interpretations of intermolecular FRET studies can be complicated. There are controversies concerning whether G proteins dissociate from the GPCR following activation and whether a GPCR/G protein complex preassembles (Janetopoulos *et al.*, 2001; Bunemann *et al.*, 2003; Hein *et al.*, 2005; Nobles *et al.*, 2005). This intermolecular FRET strategy can be extended to monitor GPCR interactions with other important regulatory proteins such as β-arrestins, revealing differential kinetics and timing between GPCR activation and inactivation (Vilardaga et al., 2003). It has also been used to monitor downstream targets such as G protein gated inwardly rectifying potassium channels (GIRKs), combining FRET imaging and electrophysiology to provide evidence for a G protein-mediated GIRK dose response (Hommers et al., 2010).

Intermolecular FRET has been used extensively to monitor the activation dynamics of metabotropic glutamate receptors (mGluRs) and $GABA_B$ receptors. These GPCRs have large extracellular ligand binding domains and function as receptor dimers (Kunishima et al., 2000). Ligand binding causes conformational changes in the extracellular domains that are transduced to the intracellular domains. By inserting CFP and YFP into intracellular loops of separate receptors of a receptor dimer, a ligand-induced conformational change can cause a change in FRET efficiency. Hence, mGluR and $GABA_B$ receptor activation can be optically monitored (Tateyama *et al.*, 2004; Matsushita *et al.*, 2010). Using this imaging strategy, the activation kinetics of mGluR1β were measured. Despite the slow signaling downstream from mGluR activation as compared to an ionotropic receptor, mGluR1β activation itself is fast, suggesting that downstream events are rate limiting (Marcaggi et al., 2009). Importantly, these kinetic parameters were used to build a model in order to evaluate the contribution of transient mGluR activation to shaping synaptic transmission. FRET imaging also showed that different ligands can induce distinct structural changes, resulting in distinct downstream G protein signaling. mGluR1α activation by glutamate or the exogenous ligand Gd^{3+} was imaged. Activation by the two ligands show different FRET responses, and the downstream responses are different. Glutamate increases both intracellular calcium and cAMP levels, but Gd^{3+} increases only the calcium levels. The imaging data suggest that glutamate activates both $G_{\alpha s}$ and $G_{\alpha q}$, but Gd^{3+} only activates $G_{\alpha q}$ (Tateyama et al., 2004).

An alternative FRET imaging strategy exploits a relative movement between the third intracellular loop and C-terminus of GPCRs (Lohse et al., 2007). With CFP inserted into Loop III and a YFP into the C-terminus, activation of the GPCR causes a decrease in FRET efficiency (Vilardaga *et al.*, 2003; Rochais *et al.*, 2007). This strategy no longer makes assumptions about the preassembly of the signaling complex, a controversial issue. Both intermolecular and intramolecular FRET strategies have been used in conjunction with electrophysiology to conduct a comprehensive study of the kinetic steps in M1 muscarinic

acetylcholine receptor (M1 mAChR) activation, downstream PLC activation, and subsequent inhibition of Kv7.2/7.3 M currents (Jensen et al., 2009). By systematically tagging different components of the M1 mAChR-$G_{\alpha\beta\gamma}$-PLC pathway, imaging data suggest that PIP_2 hydrolysis is rate-limiting due to the expression levels of PLC rather than the intrinsic kinetics of PLC. Furthermore, kinetic parameters measured in the imaging experiments were used to build a kinetic model, facilitating a quantitative comparison of the empirical observations (Jensen *et al.*, 2009; Falkenburger *et al.*, 2010).

Lipid Metabolism Linked Signaling: PIPs, IPs, DAG

Downstream from GPCR activation, metabolism of phosphoinositide lipids is intimately linked to intracellular signaling. Phosphoinositides can be hydrolyzed to inositol phosphates and diacylglycerol (DAG) in a receptor-mediated manner, and these phospholipid metabolites can subsequently modulate ion channel activity, synaptic transmission, and plasticity. To better dissect this GPCR-related signaling branch, several translocation GEIs have been developed.

Pleckstrin homology (PH) domains have been extensively used as sensing motifs to construct translocation GEIs of PIP_2 (Varnai and Balla, 2006). For example, the PH domain from phospholipase C δ1 has been fused to EGFP ($PH_{PLC\delta1}$-EGFP) to create a translocation probe. $PH_{PLC\delta1}$-EGFP binds PIP_2 in the membrane, but upon PIP_2 hydrolysis to DAG and inositol-(1,4,5)-trisphosphate (IP_3), $PH_{PLC\delta1}$-EGFP translocates to the cytoplasm (Stauffer *et al.*, 1998; Varnai and Balla, 1998). The $PH_{PLC\delta1}$-EGFP construct has been used in neuroblastoma cells and cultured hippocampal, striatal, and cerebellar granule neurons to study PLC regulation of muscarinic receptors and mGluRs (van der Wal *et al.*, 2001; Xu *et al.*, 2003; Billups *et al.*, 2006; Willets *et al.*, 2007; Kumar *et al.*, 2008; Butcher *et al.*, 2009). It has also recently been applied in organotypic brain slice to verify that carbachol can induce PIP_2 hydrolysis in cortical pyramidal neurons (Yan et al., 2009). In an early study, activity-dependent PIP_2 metabolism was visualized at presynaptic terminals in cultured hippocampal neurons (Micheva et al., 2001). A combination of $PH_{PLC\delta1}$-EGFP and FM4-64 live-cell imaging with post-hoc immunochemistry suggested that postsynaptic NMDAR activation is involved in activity-dependent PIP_2 metabolism at the presynaptic terminal.

It has been observed, however, that $PH_{PLC\delta1}$-EGFP has a 20-fold higher selectivity for IP_3, and therefore translocation following PIP_2 hydrolysis is primarily due to increased cytosolic IP_3 (Hirose et al., 1999). Taken into account, this GEI can then be used to monitor IP_3 metabolism (Okubo et al., 2001), or an alternative sensing domain can be sought. To this end, the Tubby domain, a PIP_2-binding motif of a mammalian transcription factor, was found to be selective for PIP_2 and insensitive to IP_3 (Santagata *et al.*, 2001; Quinn *et al.*, 2008; Szentpetery *et al.*, 2009). The Tubby-EGFP probe translocates to the cytoplasm due to PIP_2 hydrolysis and not to increased cytosolic IP_3.

FRET-based GEIs selective for IP_3 have also been developed using the ligand binding domains of IP_3 receptors in order to overcome the sensitivity of PH domains to both PIP_2 and IP_3 (Tanimura *et al.*, 2004; Sato *et al.*, 2005; Matsu-ura *et al.*, 2006; Remus *et al.*, 2006). These probes have been useful for specifically investigating the kinetics of IP_3 production at the plasma membrane, in the cytosol, and even in the dendrites of cultured hippocampal neurons following mAChR or mGluR activation (Tanimura *et al.*, 2004; Sato *et al.*, 2005).

Finally, translocation and FRET-based DAG selective GEIs have been engineered. These GEIs exploit the DAG-dependent membrane association of the C1 domains of protein kinase C (PKC) γ and β (Oancea *et al.*, 1998; Violin *et al.*, 2003; Nishioka *et al.*, 2008). The DAGR sensor combines both DAG-dependent translocation and environmentally sensitive FRET for a quantitative fluorescence response. DAGR is a intramolecular FRET construct

in which the C1 domains of PKCβII are sandwiched between CFP and Citrine. In contrast to the PH and Tubby probes, increased DAG in the membrane causes translocation of DAGR from the cytosol to the membrane. The membrane environment adds additional conformational constraints on the relative orientation and distance between the FPs, causing an increase in FRET associated with translocation (Violin et al., 2003). DAGR has been used in single astrocytes, for example, to demonstrate that PLCε is necessary for thrombin-induced DAG production and that carbachol-induced DAG production occurs independently because separate PLCs are activated (Citro et al., 2007).

These GEIs form a useful family of sensors that can be used to monitor the timing of GPCR modulation of synaptic activity. For example, the entire set of $PH_{PLC\delta1}$-EGFP, Tubby-EGFP, and $C1_{PKC\gamma}$-EGFP GEIs was used to dissect the kinetics of Ca^{2+}-dependent changes in PIP_2/IP_3, PIP_2, and DAG concentrations in SH-SY5Y neuroblastoma cells and cultured hippocampal neurons after stimulation of mAChRs (Nelson et al., 2008). By combining imaging and electrophysiology, these GEIs have also been extensively used to study GPCR-mediated PLC modulation of Kv7.2/7.3 M-currents, K_{ATP} currents, and TRPV2 currents (Suh *et al.*, 2004; Quinn *et al.*, 2008; Jensen *et al.*, 2009; Mercado *et al.*, 2010). In one comprehensive study of PLC regulation of M-currents, PIP_2/IP_3/DAG metabolism was imaged with $PH_{PLC\delta1}$-EGFP and $C1A_{PKC}$-EGFP, Ca^{2+} was also imaged, and electrophysiology was conducted in a series of parallel experiments. The combined data demonstrated that Ca^{2+} is required and that there is a feedback loop for PLC regulation of Kv7.2/7.3 currents (Horowitz et al., 2005).

Cyclic Nucleotides and Downstream Kinases

Cyclic nucleotides such as cyclic adenosine monophosphate (cAMP) and cyclic guanosine monophosphate (cGMP) are well-known second messengers in intracellular signaling cascades. Their temporal and spatial dynamics are highly regulated to ensure normal physiology, and many GEIs have been engineered for live-cell imaging of cAMP, cGMP, and their downstream signaling cascades (Vincent *et al.*, 2008; Willoughby and Cooper, 2008). Most of these GEIs are FRET-based. Initial sensors used intermolecular FRET strategies (Zaccolo et al., 2000), but recent sensors have used an intramolecular FRET strategy to provide a more quantitative and robust fluorescence readout.

There are several intramolecular FRET-based GEIs for imaging cAMP. For instance, a cAMP-binding protein Epac has been used as the scaffold between a FRET pair, and changes in the FRET response report changes in cAMP levels (DiPilato *et al.*, 2004; Nikolaev *et al.*, 2004). Furthermore, transgenic animals have been made for *in vivo* imaging of cAMP dynamics in intact networks. For example, Epac1-camps has been stably expressed in *Drosophila* neurons to study how neuropeptides modulate the clock network via cAMP-dependent signaling (Shafer et al., 2008)

Protein kinase activities downstream from cAMP can also be monitored with GEIs. To report the activity of the downstream cAMP-dependent protein kinase A (PKA), a cognate peptide substrate and a binding domain have been used as the scaffold between a FRET pair. Upon PKA phosphorylation of the cognate peptide, its subsequent interaction with the adjacent binding domain changes the FRET response (Nagai *et al.*, 2000; Zhang *et al.*, 2001). Imaging two GEIs, ICUE2 for cAMP and AKAR2 for PKA activity, has been used to study oscillations in second-messenger signaling cascades in dissociated cultures of retinal neurons (Dunn et al., 2006). Furthermore, using viral delivery of the AKAR2 reporter, nuclear and cytosolic PKA dynamics have been studied in individual neurons in mouse brain slice preparations (Gervasi et al., 2007). Similar to GEIs for PKA, by choosing different cognate peptide and binding domains, sensors of other protein kinases, such as Akt/protein

kinase B, protein kinase C, and AMP-dependent protein kinase, have been generated (Sasaki *et al.*, 2003; Violin *et al.*, 2003; Tsou *et al.*, 2011). Their signals often reflect a balance between the phosphorylation reaction by the kinase and the dephosphorylation reaction by cellular phosphatases. When using these GEIs, it is important to validate their sensitivity and specificity (Vincent et al., 2008), and a GEI variant with spoiled phosphorylation site is often a useful negative control.

To report cellular cGMP dynamics, FRET-based and cpFP-based GEIs have been designed (Honda *et al.*, 2001; Nausch *et al.*, 2008). Furthermore, to detect the upstream signaling molecule nitric oxide (NO), a FRET-based cGMP reporter can be used in combination with soluble guanylate cyclase, a nitric oxide (NO)-dependent enzyme; exposure to minute NO leads to formation of several cGMP molecules and thus amplifies the fluorescent signal. This amplification scheme has been used to detect picomolar NO released from cultured hippocampal neurons (Sato et al., 2006).

Small GTPases

Small GTPases regulate cytoskeletal dynamics at the neurite growth cone (Dickson, 2001). Small GTPases are G proteins that function similar to the α-subunits of heterotrimeric G-proteins. Small GTPases can be activated by exchange of GTP for GDP, promoted by guanine nucleotide exchange factors, and they are inactivated when GTP is hydrolyzed to GDP, promoted by GTPase activating proteins. To image the activated conformation of a small GTPase, one successful strategy uses the target GTPase and a binding partner labeled with the respective partners of a FRET pair. The binding partner selectively recognizes the GTP-bound, activated conformation of the GTPase, leading to a dynamic FRET signal that provides a readout for activation (Kraynov et al., 2000). This strategy has been adapted to engineer GEIs based on intramolecular FRET, and sensors have been developed to detect the activation of Ras and Rho family members – Ras, Rap1, RhoA, Rac, Cdc42 – as well as for other small GTPases (Mochizuki *et al.*, 2001; Itoh *et al.*, 2002; Yoshizaki *et al.*, 2003; Pertz *et al.*, 2006; Aoki *et al.*, 2008; Sabouri-Ghomi *et al.*, 2008).

Neurite outgrowth in the PC12 cell line has been examined extensively using GEIs for Ras and Rho small GTPases (Nakamura et al., 2008). The Raichu series of GEIs allow neurite outgrowth to be monitored in parallel with G protein activity, revealing signaling requirements for the successful action of outgrowth signals such as nerve growth factor or dibutyryl-cAMP (Goto et al., 2011). Quantitative live-cell imaging has also provided spatial and temporal parameters characterizing the Rac1 and cdc42 signaling pathway for neurite outgrowth (Aoki *et al.*, 2004; Aoki *et al.*, 2005; Aoki *et al.*, 2007). These parameters were used to create a signaling model, predicting that a PI-5phophatase negatively regulates outgrowth (Aoki et al., 2007). Experimental verification of this prediction shows that this type of quantitative analysis and modeling may provide valuable insights into the convergence and divergence of signaling pathways governing neurite outgrowth and guidance.

These GEIs have also been used to show that Rac and RhoA regulate dendritic spine morphogenesis in cultured hippocampal neurons. Both overexpression of a constitutively active RhoA mutant and knockdown of the polarity protein PAR-6 inhibit dendritic spine formation. Imaging the Raichu GEI for RhoA demonstrated that PAR-6 knockdown caused increased RhoA activity, suggesting that PAR-6 promotes spine morphogenesis by negative upstream regulation of RhoA (Zhang and Macara, 2008). Similarly, imaging Rac activity suggested a delineation of several steps of NMDAR regulation of spine morphogenesis. The guanine nucleotide exchange factor PIX activates Rac, and PIX interaction with Rac is promoted by CaMKK/CaMKI. Ras imaging showed that Ras activity in dendritic spines can

be increased by depolarization in a CaMK dependent manner, and overexpression of a phosphorylation deficient PIX dominant negative can attenuate activation (Saneyoshi et al., 2008). These imaging data may suggest that NMDAR activation causes calcium influx and CaMK activation, and these signaling events could lead to local phosphorylation of PIX and subsequently local activation of Rac to promote spine morphogenesis.

Imaging RhoA activity in cultured cortical neurons and in brain slices has also shown that the subcellular localization of RhoA activation is important for the regulation of cortical neuron migration during development (Pacary et al., 2011). The regulatory proteins Rnd2 and Rnd3 promote neuronal migration by inhibiting RhoA activity, but knockdown has different pathological phenotypes. In this study, Raichu was genetically targeted to different subcellular compartments, and imaging RhoA activity demonstrated that only Rnd3 knockdown increases RhoA activity at the plasma membrane. The spatial resolution resulting from this strategy was instrumental for showing that spatial organization of RhoA activity existed and that compartmentation of signaling components may be a key regulatory feature in neuronal migration.

Proteases

Protease activity regulates numerous signaling events including neuronal cell death, and FRET-based GEIs have long been used to monitor proteolytic cleavage of substrates. Sensors of proteolysis can be created by fusing a FRET pair using a peptide linker that contains recognition and cleavage sites. For example, FRET-based GEIs containing the Asp-Glu-Val-Asp (DEVD) caspase cleavage sequence have been used to monitor apoptosis (Xu et al., 1998). In the absence of caspase activity, the FPs remain covalently attached, and their close proximity results in a high FRET state. Upon proteolytic cleavage, the FPs can diffuse away from one another resulting in a loss of FRET, indicating caspase activation and apoptosis.

These FRET-based GEIs of protease activities have greatly complemented biochemical and genetic techniques in the study of neuronal cell death. GEIs containing the DEVD cleavage site have been used to investigate the role of the Puma, a BH3-only proapoptotic protein, in caspase dependent and independent neuronal cell death (Tuffy et al., 2010). The DEVD cleavage site can also be replaced by other cleavage motifs, and the cleavage domain can even be an entire protein such as the full-length BID protein, another BH3-only proapoptotic protein (Ward et al., 2006). Glutamate excitotoxicity can induce caspase cleavage of full-length BID, and the truncated BID product can activate mitochondrial apoptosis pathways. Imaging a CFP-BID-YFP construct revealed the kinetics of caspase proteolysis of BID as well as the translocation of both full-length and truncated BID to mitochondria in cerebellar granule neurons (Ward et al., 2006).

Glutamate receptor activation can also lead to activation of other proteases such as calpains. Calpains are Ca^{2+}-dependent proteases, and two types have been identified that have micromolar (μ-calpain) and millimolar (m-calpain) affinity for Ca^{2+}. Calcium influx following synaptic activity has been proposed to activate calpains, causing proteolytic cleavage of cytoskeletal, receptor, and cytosolic substrates. The identity of these substrates suggests that calpain activity may modulate morphology, synaptic plasticity, and cell death (Zadran et al., 2010). A GEI of calpain activity was designed using a fusion between ECFP and EYFP linked by the calpain recognition site from α-spectrin (Vanderklish et al., 2000). The sensor was also targeted to postsynaptic dendritic spines using the Shaker PDZ domain. Imaging this sensor in cultured hippocampal neurons and organotypic hippocampal slices revealed that activation of glutamate receptors decreases FRET within minutes, demonstrating activity-dependent calpain activation (Vanderklish et al., 2000). Imaging

experiments also showed that chronic glutamate exposure causes a large sustained increase in cytosolic Ca^{2+} that precedes calpain activation. These imaging data suggest that calpain cleavage of the sodium-calcium exchanger is not responsible for the loss of calcium homeostasis and eventually cell death, as had been previously hypothesized (Gerencser et al., 2009).

Reactive Oxygen Species and Redox Potential

Reactive oxygen species (ROS) and free radicals are generated in diverse metabolic processes, and they can often act as messengers in signal transduction by altering the reduction-oxidation (redox) status of various signaling proteins (Winterbourn, 2008). Considering the importance of ROS and redox signaling in cellular physiology, numerous chemical-based probes (Wardman, 2007) and genetically encoded GFP-based biosensors (Meyer and Dick, 2010) have been devised. These reporters can assess either the cellular redox status in general, or a particular ROS or redox metabolite.

As reporters of general cellular redox status, redox-sensitive yellow FPs (rxYFPs) (Ostergaard et al., 2001) and redox-sensitive green FPs (roGFPs) (Hanson et al., 2004) have been created by engineering two surface-exposed cysteine residues near the chromophore. The thiol oxidation status of these cysteines is influenced by cellular oxidants and antioxidants, and redox status affects the FP conformation and the fluorescence response. Compared with the rxYFP reporter, roGFP is more commonly used for two reasons: first, unlike rxYFP, roGFP is ratiometric and thus provides a more quantitative measurement; second, some roGFP variants are notably pH resistant (Meyer and Dick, 2010), while rxYFP is pH sensitive in the physiological pH range (Ostergaard et al., 2001). By using targeting sequences to various cellular compartments, these redox-sensitive reporters can report the general redox states of mitochondria, nuclei, and endoplasmic reticulum (Dooley *et al.*, 2004; Merksamer *et al.*, 2008), and the GEIs have been expressed in dissociated neuronal cultures for bioenergetics studies (Vesce et al., 2005). In addition, transgenic mice have been generated to express the mito-roGFP biosensor under the control of the tyrosine hydroxylase promoter. By imaging acute brain slices with two-photon microscopy, mitochondrial oxidant stress levels were monitored in substantia nigra dopaminergic neurons during activity (Guzman et al., 2010).

Although roGFP variants have undefined redox specificity, other fluorescent sensors have been engineered to address this issue by linking GFP variants to specific ROS binding protein domains. For instance, a fluorescent reporter of hydrogen peroxide, named HyPer, has been created by linking a cpYFP to a bacterial H_2O_2 binding domain OxyR (Belousov et al., 2006). Unfortunately, HyPer is very pH sensitive like many cpFP-based GEIs, and a pH fluctuation of 0.3 units can mimic the entire excursion of the sensor response. It is thus important to monitor pH to correct for artifacts in the sensor measurements. Fortuitously, it has been found that cpYFP by itself, even with no linkage to any ligand binding domains, could report superoxide. While cpYFP has been exploited to monitor superoxide burst in single mitochondria (Wang et al., 2008b), it is unclear how superoxide interacts with the cpYFP chromophore, and whether this interaction is specific for superoxide.

In addition to ligand binding domains, redox enzymes can be linked to GFP variants to create fluorescent reporters with defined redox specificity. For instance, while roGFP2 by itself reports the general cellular redox status, by linking roGFP2 to a human thioltransferase Grx1, a fluorescent reporter specific for glutathione redox has been created (Gutscher et al., 2008). Not only is Grx1-roGFP2 pH resistant, but it is also fast in its response to changes in glutathione redox. Using a similar strategy, fluorescent sensors of other redox equilibria can be created as well (Gutscher et al., 2009).

Challenges for Using GEIs

We believe that GEIs provide a unique and powerful method for monitoring neuronal and glial activity in live cells, but there are many important challenges for using GEIs that should be reiterated, including specificity and expression induced pathophysiology.

Engineering and validating the specificity of a GEI is both a critical and non-trivial task in sensor development. As mentioned throughout this review, pH sensitivity is a pervasive problem for GEI specificity. Many GEIs are significantly pH sensitive and require correction in order to discriminate real changes of interest from signal artifacts caused by pH changes (Berg *et al.*, 2009). pH is not the only culprit, however, and many other environmental factors can cause signal artifacts or changes in a GEI's sensing characteristics (Willemse *et al.*, 2007; Takanaga *et al.*, 2008). For example, interpretation of cpYFP responses in mitochondria as an indication of superoxide flashes (Wang *et al.*, 2008b) has been questioned because of alternative interpretations of pharmacological data (Muller, 2009) and the inherent pH sensitivity of the probe (Schwarzlander *et al.*, 2011). This case illustrates how, even with significant sensor characterization (Wang *et al.*, 2008b), questions of specificity can arise as the GEI is used, and equivocal sensing behavior may merit deeper investigation. Therefore, due diligence in the characterization of interferences *in vitro* and in the validation of specificity *in vivo* is required in order to establish GEIs as reliable tools in neurobiology, otherwise uncertainty over the specificity of a GEI can cause confusion and controversy over the interpretation of data.

Pathophysiology induced by expression of GEIs is also an undesired outcome that should be considered. As previously mentioned, alteration or interaction with endogenous signaling pathways by expressed GEIs can seriously compromise the utility of a reporter (e.g. GEIs that buffer low level analytes or bind signaling proteins with greater occupancy than endogenous binding partners). It is always possible that the expression of a foreign protein can have unexpected and unwanted effects on the anatomy and physiology of the system. While GFPs have generally been shown and assumed to be inert reporters *in vitro* and *in vivo* (Feng *et al.*, 2000; Zuo *et al.*, 2004), there are several examples in the literature demonstrating that the innocuousness of GFP or GEI expression should be explicitly tested. Early reports indicated that overexpression of GFP in cell lines can be cytotoxic with increased apoptosis (Hanazono *et al.*, 1997; Liu *et al.*, 1999). Targeted expression of GFP can cause fatal cardiomyopathy in mice (Huang *et al.*, 2000), and GFP has been shown to interfere with excitation-contraction coupling by interacting with myosin (Agbulut *et al.*, 2006). It has also been reported that GFP can unexpectedly attenuate NFκB signaling and polyubiquitination (Baens *et al.*, 2006). Importantly, GFP expression in the brain can increase the expression of stress response associated genes (Comley *et al.*, 2011) and may be neurotoxic causing significant neuronal death (Krestel *et al.*, 2004; Klein *et al.*, 2006). These examples serve as a reminder that all observation methods, including optical monitoring of GEIs, perturb the system to some extent. While the literature suggests that GFP and GEIs can be used with minimal perturbation of cellular function, explicit experimental validation of this supposition should not be neglected.

Finally, and most trivially, low fluorescence or small fluorescence changes can be a practical limitation on the use of many GEIs in cells: the real-world signal-to-noise in the presence of instrumentation noise and background fluorescence may just be too small for detecting subtle changes in the physiological targets of the indicators.

Future Directions

Many GEIs have been engineered for monitoring metabolic and signaling dynamics in the brain. While these provide a significant tool set, it is far from complete. Obviously,

continued engineering of new GEIs for different targets is a major challenge. Compared to the tens of thousands of unique metabolites and proteins, currently only a tiny fraction can be directly imaged with GEIs. While some general design principles have emerged, numerous challenges remain in the engineering and application of GEIs. These challenges extend to all levels of the methodology from basic FP chemistry up to systems level modeling.

There is no doubt that GEI development will benefit from an increased understanding of FP chemistry and photophysics. Biological factors such as changing pH and ROS levels are unavoidable, and a mechanistic understanding of how these factors affect FP fluorescence will aid the optimization of GEIs. Likewise, a mechanistic understanding of photophysical properties such as photoconversion, photobleaching, and photoisomerization will hopefully lead to the continued engineering of new FPs with improved characteristics. The development of new FP color variants will also greatly facilitate the diversification of GEI color schemes, a key requirement for multiplex imaging of several GEIs simultaneously.

It will also be important to promote the development of multiphoton microscopy techniques for imaging of GEIs in thick samples and *in vivo*. Combining GEIs with multiphoton imaging can be a powerful, non-invasive method for visualizing signaling dynamics in intact networks (Svoboda and Yasuda, 2006). Alternative methods such as two-photon fluorescence lifetime microscopy also show promise for quantitative imaging of FPs and GEIs *in vivo* (Drobizhev *et al.*, 2011). Hopefully, the techniques and instrumentation will become more accessible so that imaging experiments can be carried out more routinely in live animals, providing better physiological parameters.

Finally, quantitative analysis of data from parallel imaging studies will be important for building systems level models. Models can provide a great deal of insight into the control and behavior of intricate metabolic and signaling networks, but models are limited by the empirical parameters they are built from. Imaging GEIs *in vivo* will be a critical step in building physiologically relevant models of brain function.

Conclusion

Fluorescent protein based sensors provide a powerful tool for quantitative live-cell imaging, and consequently the field of protein engineering and genetically-encoded indicators has grown immensely. Here, we have outlined several design strategies for the development of genetically-encoded indicators, and we have provided several examples of their use in brain-related studies. These sensors provide a high level of spatial and temporal resolution, and the ability to monitor signaling dynamics on either the single-cell or population level has revealed many new details about biological networks. While the development and optimization of new sensors can require several years of engineering work, we believe the payoff is well worth the effort.

Acknowledgments

M.T. is supported by a Postdoctoral Fellowship from the NIH (F32NS066613), and this work was supported by a research grant from the NIH (R01NS055031) to G.Y.

References

Agbulut O, Coirault C, Niederlander N, Huet A, Vicart P, Hagege A, Puceat M, Menasche P. GFP expression in muscle cells impairs actin-myosin interactions: implications for cell therapy. Nat Methods. 2006; 3:331. [PubMed: 16628201]

Akerboom J, Rivera JD, Guilbe MM, Malave EC, Hernandez HH, Tian L, Hires SA, Marvin JS, Looger LL, Schreiter ER. Crystal structures of the GCaMP calcium sensor reveal the mechanism of fluorescence signal change and aid rational design. J Biol Chem. 2009; 284:6455–6464. [PubMed: 19098007]

Aoki K, Kiyokawa E, Nakamura T, Matsuda M. Visualization of growth signal transduction cascades in living cells with genetically encoded probes based on Forster resonance energy transfer. Philos Trans R Soc Lond B Biol Sci. 2008; 363:2143–2151. [PubMed: 18343776]

Aoki K, Nakamura T, Fujikawa K, Matsuda M. Local phosphatidylinositol 3,4,5-trisphosphate accumulation recruits Vav2 and Vav3 to activate Rac1/Cdc42 and initiate neurite outgrowth in nerve growth factor-stimulated PC12 cells. Mol Biol Cell. 2005; 16:2207–2217. [PubMed: 15728722]

Aoki K, Nakamura T, Inoue T, Meyer T, Matsuda M. An essential role for the SHIP2-dependent negative feedback loop in neuritogenesis of nerve growth factor-stimulated PC12 cells. J Cell Biol. 2007; 177:817–827. [PubMed: 17535963]

Aoki K, Nakamura T, Matsuda M. Spatio-temporal regulation of Rac1 and Cdc42 activity during nerve growth factor-induced neurite outgrowth in PC12 cells. J Biol Chem. 2004; 279:713–719. [PubMed: 14570905]

Azarias G, Perreten H, Lengacher S, Poburko D, Demaurex N, Magistretti PJ, Chatton JY. Glutamate transport decreases mitochondrial pH and modulates oxidative metabolism in astrocytes. J Neurosci. 2011; 31:3550–3559. [PubMed: 21389211]

Baens M, Noels H, Broeckx V, Hagens S, Fevery S, Billiau AD, Vankelecom H, Marynen P. The dark side of EGFP: defective polyubiquitination. PLoS One. 2006; 1:e54. [PubMed: 17183684]

Baird GS, Zacharias DA, Tsien RY. Circular permutation and receptor insertion within green fluorescent proteins. Proc Natl Acad Sci USA. 1999; 96:11241–11246. [PubMed: 10500161]

Belousov VV, Fradkov AF, Lukyanov KA, Staroverov DB, Shakhbazov KS, Terskikh AV, Lukyanov S. Genetically encoded fluorescent indicator for intracellular hydrogen peroxide. Nat Methods. 2006; 3:281–286. [PubMed: 16554833]

Berg J, Hung YP, Yellen G. A genetically encoded fluorescent reporter of ATP:ADP ratio. Nat Methods. 2009; 6:161–166. [PubMed: 19122669]

Berglund K, Schleich W, Krieger P, Loo LS, Wang D, Cant NB, Feng G, Augustine GJ, Kuner T. Imaging synaptic inhibition in transgenic mice expressing the chloride indicator, Clomeleon. Brain Cell Biol. 2006; 35:207–228. [PubMed: 18398684]

Berglund K, Schleich W, Wang H, Feng G, Hall WC, Kuner T, Augustine GJ. Imaging synaptic inhibition throughout the brain via genetically targeted Clomeleon. Brain Cell Biol. 2008; 36:101–118. [PubMed: 18850274]

Billups D, Billups B, Challiss RA, Nahorski SR. Modulation of Gq-protein-coupled inositol trisphosphate and Ca2+ signaling by the membrane potential. J Neurosci. 2006; 26:9983–9995. [PubMed: 17005862]

Bittner CX, Loaiza A, Ruminot I, Larenas V, Sotelo-Hitschfeld T, Gutierrez R, Cordova A, Valdebenito R, Frommer WB, Barros LF. High resolution measurement of the glycolytic rate. Front Neuroenergetics. 2010; 2:26. [PubMed: 20890447]

Bittner CX, Valdebenito R, Ruminot I, Loaiza A, Larenas V, Sotelo-Hitschfeld T, Moldenhauer H, San Martin A, Gutierrez R, Zambrano M, Barros LF. Fast and reversible stimulation of astrocytic glycolysis by k+ and a delayed and persistent effect of glutamate. J Neurosci. 2011; 31:4709–4713. [PubMed: 21430169]

Bizzarri R, Serresi M, Luin S, Beltram F. Green fluorescent protein based pH indicators for in vivo use: a review. Anal Bioanal Chem. 2009; 393:1107–1122. [PubMed: 19034433]

Bunemann M, Frank M, Lohse MJ. Gi protein activation in intact cells involves subunit rearrangement rather than dissociation. Proc Natl Acad Sci USA. 2003; 100:16077–16082. [PubMed: 14673086]

Butcher AJ, Torrecilla I, Young KW, Kong KC, Mistry SC, Bottrill AR, Tobin AB. N-methyl-D-aspartate receptors mediate the phosphorylation and desensitization of muscarinic receptors in cerebellar granule neurons. J Biol Chem. 2009; 284:17147–17156. [PubMed: 19332541]

Casey JR, Grinstein S, Orlowski J. Sensors and regulators of intracellular pH. Nat Rev Mol Cell Biol. 2010; 11:50–61. [PubMed: 19997129]

Chesler M, Kaila K. Modulation of pH by neuronal activity. Trends Neurosci. 1992; 15:396–402. [PubMed: 1279865]

Chudakov DM, Matz MV, Lukyanov S, Lukyanov KA. Fluorescent proteins and their applications in imaging living cells and tissues. Physiol Rev. 2010; 90:1103–1163. [PubMed: 20664080]

Ciruela F, Vilardaga JP, Fernandez-Duenas V. Lighting up multiprotein complexes: lessons from GPCR oligomerization. Trends Biotechnol. 2010; 28:407–415. [PubMed: 20542584]

Citro S, Malik S, Oestreich EA, Radeff-Huang J, Kelley GG, Smrcka AV, Brown JH. Phospholipase Cepsilon is a nexus for Rho and Rap-mediated G protein-coupled receptor-induced astrocyte proliferation. Proc Natl Acad Sci USA. 2007; 104:15543–15548. [PubMed: 17878312]

Comley LH, Wishart TM, Baxter B, Murray LM, Nimmo A, Thomson D, Parson SH, Gillingwater TH. Induction of cell stress in neurons from transgenic mice expressing yellow fluorescent protein: implications for neurodegeneration research. PLoS One. 2011; 6:e17639. [PubMed: 21408118]

Day RN, Davidson MW. The fluorescent protein palette: tools for cellular imaging. Chem Soc Rev. 2009; 38:2887–2921. [PubMed: 19771335]

Deuschle K, Okumoto S, Fehr M, Looger LL, Kozhukh L, Frommer WB. Construction and optimization of a family of genetically encoded metabolite sensors by semirational protein engineering. Protein Sci. 2005; 14:2304–2314. [PubMed: 16131659]

Dickson BJ. Rho GTPases in growth cone guidance. Curr Opin Neurobiol. 2001; 11:103–110. [PubMed: 11179879]

DiPilato LM, Cheng X, Zhang J. Fluorescent indicators of cAMP and Epac activation reveal differential dynamics of cAMP signaling within discrete subcellular compartments. Proc Natl Acad Sci USA. 2004; 101:16513–16518. [PubMed: 15545605]

Dittmer PJ, Miranda JG, Gorski JA, Palmer AE. Genetically encoded sensors to elucidate spatial distribution of cellular zinc. J Biol Chem. 2009; 284:16289–16297. [PubMed: 19363034]

Dooley CT, Dore TM, Hanson GT, Jackson WC, Remington SJ, Tsien RY. Imaging dynamic redox changes in mammalian cells with green fluorescent protein indicators. J Biol Chem. 2004; 279:22284–22293. [PubMed: 14985369]

Drobizhev M, Makarov NS, Tillo SE, Hughes TE, Rebane A. Two-photon absorption properties of fluorescent proteins. Nat Methods. 2011; 8:393–399. [PubMed: 21527931]

Duebel J, Haverkamp S, Schleich W, Feng G, Augustine GJ, Kuner T, Euler T. Two-photon imaging reveals somatodendritic chloride gradient in retinal ON-type bipolar cells expressing the biosensor Clomeleon. Neuron. 2006; 49:81–94. [PubMed: 16387641]

Dulla C, Tani H, Okumoto S, Frommer WB, Reimer RJ, Huguenard JR. Imaging of glutamate in brain slices using FRET sensors. J Neurosci Methods. 2008; 168:306–319. [PubMed: 18160134]

Dunn TA, Wang CT, Colicos MA, Zaccolo M, DiPilato LM, Zhang J, Tsien RY, Feller MB. Imaging of cAMP levels and protein kinase A activity reveals that retinal waves drive oscillations in second-messenger cascades. J Neurosci. 2006; 26:12807–12815. [PubMed: 17151284]

Dzhala VI, Kuchibhotla KV, Glykys JC, Kahle KT, Swiercz WB, Feng G, Kuner T, Augustine GJ, Bacskai BJ, Staley KJ. Progressive NKCC1-dependent neuronal chloride accumulation during neonatal seizures. J Neurosci. 2010; 30:11745–11761. [PubMed: 20810895]

Falkenburger BH, Jensen JB, Hille B. Kinetics of M1 muscarinic receptor and G protein signaling to phospholipase C in living cells. J Gen Physiol. 2010; 135:81–97. [PubMed: 20100890]

Fehr M, Lalonde S, Lager I, Wolff MW, Frommer WB. In vivo imaging of the dynamics of glucose uptake in the cytosol of COS-7 cells by fluorescent nanosensors. J Biol Chem. 2003; 278:19127–19133. [PubMed: 12649277]

Feng G, Mellor RH, Bernstein M, Keller-Peck C, Nguyen QT, Wallace M, Nerbonne JM, Lichtman JW, Sanes JR. Imaging neuronal subsets in transgenic mice expressing multiple spectral variants of GFP. Neuron. 2000; 28:41–51. [PubMed: 11086982]

Fernandez-Alfonso T, Ryan TA. The kinetics of synaptic vesicle pool depletion at CNS synaptic terminals. Neuron. 2004; 41:943–953. [PubMed: 15046726]

Frederickson CJ, Koh JY, Bush AI. The neurobiology of zinc in health and disease. Nat Rev Neurosci. 2005; 6:449–462. [PubMed: 15891778]

Frommer WB, Davidson MW, Campbell RE. Genetically encoded biosensors based on engineered fluorescent proteins. Chem Soc Rev. 2009; 38:2833–2841. [PubMed: 19771330]

Gandhi SP, Stevens CF. Three modes of synaptic vesicular recycling revealed by single-vesicle imaging. Nature. 2003; 423:607–613. [PubMed: 12789331]

Gerencser AA, Mark KA, Hubbard AE, Divakaruni AS, Mehrabian Z, Nicholls DG, Polster BM. Real-time visualization of cytoplasmic calpain activation and calcium deregulation in acute glutamate excitotoxicity. J Neurochem. 2009; 110:990–1004. [PubMed: 19493161]

Gervasi N, Hepp R, Tricoire L, Zhang J, Lambolez B, Paupardin-Tritsch D, Vincent P. Dynamics of protein kinase A signaling at the membrane, in the cytosol, and in the nucleus of neurons in mouse brain slices. J Neurosci. 2007; 27:2744–2750. [PubMed: 17360896]

Glykys J, Dzhala VI, Kuchibhotla KV, Feng G, Kuner T, Augustine G, Bacskai BJ, Staley KJ. Differences in cortical versus subcortical GABAergic signaling: a candidate mechanism of electroclinical uncoupling of neonatal seizures. Neuron. 2009; 63:657–672. [PubMed: 19755108]

Goto A, Hoshino M, Matsuda M, Nakamura T. Phosphorylation of STEF/Tiam2 by protein kinase a is critical for Rac1 activation and neurite outgrowth in dibutyryl cAMP-treated PC12D cells. Mol Biol Cell. 2011; 22:1780–1790. [PubMed: 21460187]

Granseth B, Odermatt B, Royle SJ, Lagnado L. Clathrin-mediated endocytosis is the dominant mechanism of vesicle retrieval at hippocampal synapses. Neuron. 2006; 51:773–786. [PubMed: 16982422]

Griesbeck O, Baird GS, Campbell RE, Zacharias DA, Tsien RY. Reducing the environmental sensitivity of yellow fluorescent protein. Mechanism and applications. J Biol Chem. 2001; 276:29188–29194. [PubMed: 11387331]

Gutscher M, Pauleau AL, Marty L, Brach T, Wabnitz GH, Samstag Y, Meyer AJ, Dick TP. Real-time imaging of the intracellular glutathione redox potential. Nat Methods. 2008; 5:553–559. [PubMed: 18469822]

Gutscher M, Sobotta MC, Wabnitz GH, Ballikaya S, Meyer AJ, Samstag Y, Dick TP. Proximity-based protein thiol oxidation by H2O2-scavenging peroxidases. J Biol Chem. 2009; 284:31532–31540. [PubMed: 19755417]

Guzman JN, Sanchez-Padilla J, Wokosin D, Kondapalli J, Ilijic E, Schumacker PT, Surmeier DJ. Oxidant stress evoked by pacemaking in dopaminergic neurons is attenuated by DJ-1. Nature. 2010; 468:696–700. [PubMed: 21068725]

Hanazono Y, Yu JM, Dunbar CE, Emmons RV. Green fluorescent protein retroviral vectors: low titer and high recombination frequency suggest a selective disadvantage. Hum Gene Ther. 1997; 8:1313–1319. [PubMed: 9295126]

Hanson GT, Aggeler R, Oglesbee D, Cannon M, Capaldi RA, Tsien RY, Remington SJ. Investigating mitochondrial redox potential with redox-sensitive green fluorescent protein indicators. J Biol Chem. 2004; 279:13044–13053. [PubMed: 14722062]

Hanson GT, McAnaney TB, Park ES, Rendell ME, Yarbrough DK, Chu S, Xi L, Boxer SG, Montrose MH, Remington SJ. Green fluorescent protein variants as ratiometric dual emission pH sensors. 1 Structural characterization and preliminary application. Biochemistry. 2002; 41:15477–15488. [PubMed: 12501176]

Hein P, Frank M, Hoffmann C, Lohse MJ, Bunemann M. Dynamics of receptor/G protein coupling in living cells. EMBO J. 2005; 24:4106–4114. [PubMed: 16292347]

Hemmings HC Jr, Yan W, Westphalen RI, Ryan TA. The general anesthetic isoflurane depresses synaptic vesicle exocytosis. Mol Pharmacol. 2005; 67:1591–1599. [PubMed: 15728262]

Hires SA, Zhu Y, Tsien RY. Optical measurement of synaptic glutamate spillover and reuptake by linker optimized glutamate-sensitive fluorescent reporters. Proc Natl Acad Sci USA. 2008; 105:4411–4416. [PubMed: 18332427]

Hirose K, Kadowaki S, Tanabe M, Takeshima H, Iino M. Spatiotemporal dynamics of inositol 1,4,5-trisphosphate that underlies complex Ca2+ mobilization patterns. Science. 1999; 284:1527–1530. [PubMed: 10348740]

Hommers LG, Klenk C, Dees C, Bunemann M. G proteins in reverse mode: receptor-mediated GTP release inhibits G protein and effector function. J Biol Chem. 2010; 285:8227–8233. [PubMed: 20075078]

Honda A, Adams SR, Sawyer CL, Lev-Ram V, Tsien RY, Dostmann WR. Spatiotemporal dynamics of guanosine 3′,5′-cyclic monophosphate revealed by a genetically encoded, fluorescent indicator. Proc Natl Acad Sci USA. 2001; 98:2437–2442. [PubMed: 11226257]

Horowitz LF, Hirdes W, Suh BC, Hilgemann DW, Mackie K, Hille B. Phospholipase C in living cells: activation, inhibition, Ca2+ requirement, and regulation of M current. J Gen Physiol. 2005; 126:243–262. [PubMed: 16129772]

Huang WY, Aramburu J, Douglas PS, Izumo S. Transgenic expression of green fluorescence protein can cause dilated cardiomyopathy. Nat Med. 2000; 6:482–483. [PubMed: 10802676]

Imamura H, Nhat KP, Togawa H, Saito K, Iino R, Kato-Yamada Y, Nagai T, Noji H. Visualization of ATP levels inside single living cells with fluorescence resonance energy transfer-based genetically encoded indicators. Proc Natl Acad Sci USA. 2009; 106:15651–15656. [PubMed: 19720993]

Itoh RE, Kurokawa K, Ohba Y, Yoshizaki H, Mochizuki N, Matsuda M. Activation of rac and cdc42 video imaged by fluorescent resonance energy transfer-based single-molecule probes in the membrane of living cells. Mol Cell Biol. 2002; 22:6582–6591. [PubMed: 12192056]

Janetopoulos C, Jin T, Devreotes P. Receptor-mediated activation of heterotrimeric G-proteins in living cells. Science. 2001; 291:2408–2411. [PubMed: 11264536]

Jayaraman S, Haggie P, Wachter RM, Remington SJ, Verkman AS. Mechanism and cellular applications of a green fluorescent protein-based halide sensor. J Biol Chem. 2000; 275:6047–6050. [PubMed: 10692389]

Jensen JB, Lyssand JS, Hague C, Hille B. Fluorescence changes reveal kinetic steps of muscarinic receptor-mediated modulation of phosphoinositides and Kv7.2/7.3 K+ channels. J Gen Physiol. 2009; 133:347–359. [PubMed: 19332618]

Klein RL, Dayton RD, Leidenheimer NJ, Jansen K, Golde TE, Zweig RM. Efficient neuronal gene transfer with AAV8 leads to neurotoxic levels of tau or green fluorescent proteins. Mol Ther. 2006; 13:517–527. [PubMed: 16325474]

Knopfel T, Lin MZ, Levskaya A, Tian L, Lin JY, Boyden ES. Toward the second generation of optogenetic tools. J Neurosci. 2010; 30:14998–15004. [PubMed: 21068304]

Kraynov VS, Chamberlain C, Bokoch GM, Schwartz MA, Slabaugh S, Hahn KM. Localized Rac activation dynamics visualized in living cells. Science. 2000; 290:333–337. [PubMed: 11030651]

Krestel HE, Mihaljevic AL, Hoffman DA, Schneider A. Neuronal co-expression of EGFP and beta-galactosidase in mice causes neuropathology and premature death. Neurobiol Dis. 2004; 17:310–318. [PubMed: 15474368]

Kumar V, Jong YJ, O'Malley KL. Activated nuclear metabotropic glutamate receptor mGlu5 couples to nuclear Gq/11 proteins to generate inositol 1,4,5-trisphosphate-mediated nuclear Ca2+ release. J Biol Chem. 2008; 283:14072–14083. [PubMed: 18337251]

Kuner T, Augustine GJ. A genetically encoded ratiometric indicator for chloride: capturing chloride transients in cultured hippocampal neurons. Neuron. 2000; 27:447–459. [PubMed: 11055428]

Kunishima N, Shimada Y, Tsuji Y, Sato T, Yamamoto M, Kumasaka T, Nakanishi S, Jingami H, Morikawa K. Structural basis of glutamate recognition by a dimeric metabotropic glutamate receptor. Nature. 2000; 407:971–977. [PubMed: 11069170]

Lee S, Yoon BE, Berglund K, Oh SJ, Park H, Shin HS, Augustine GJ, Lee CJ. Channel-mediated tonic GABA release from glia. Science. 2010; 330:790–796. [PubMed: 20929730]

Li Z, Burrone J, Tyler WJ, Hartman KN, Albeanu DF, Murthy VN. Synaptic vesicle recycling studied in transgenic mice expressing synaptopHluorin. Proc Natl Acad Sci USA. 2005; 102:6131–6136. [PubMed: 15837917]

Liu HS, Jan MS, Chou CK, Chen PH, Ke NJ. Is green fluorescent protein toxic to the living cells? Biochem Biophys Res Commun. 1999; 260:712–717. [PubMed: 10403831]

Lohse MJ, Bunemann M, Hoffmann C, Vilardaga JP, Nikolaev VO. Monitoring receptor signaling by intramolecular FRET. Curr Opin Pharmacol. 2007; 7:547–553. [PubMed: 17919975]

Lohse MJ, Nikolaev VO, Hein P, Hoffmann C, Vilardaga JP, Bunemann M. Optical techniques to analyze real-time activation and signaling of G-protein-coupled receptors. Trends Pharmacol Sci. 2008; 29:159–165. [PubMed: 18262662]

Marcaggi P, Mutoh H, Dimitrov D, Beato M, Knopfel T. Optical measurement of mGluR1 conformational changes reveals fast activation, slow deactivation, and sensitization. Proc Natl Acad Sci USA. 2009; 106:11388–11393. [PubMed: 19549872]

Markova O, Mukhtarov M, Real E, Jacob Y, Bregestovski P. Genetically encoded chloride indicator with improved sensitivity. J Neurosci Methods. 2008; 170:67–76. [PubMed: 18279971]

Matsu-ura T, Michikawa T, Inoue T, Miyawaki A, Yoshida M, Mikoshiba K. Cytosolic inositol 1,4,5-trisphosphate dynamics during intracellular calcium oscillations in living cells. J Cell Biol. 2006; 173:755–765. [PubMed: 16754959]

Matsushita S, Nakata H, Kubo Y, Tateyama M. Ligand-induced rearrangements of the GABA(B) receptor revealed by fluorescence resonance energy transfer. J Biol Chem. 2010; 285:10291–10299. [PubMed: 20129919]

McGann JP, Pirez N, Gainey MA, Muratore C, Elias AS, Wachowiak M. Odorant representations are modulated by intra- but not interglomerular presynaptic inhibition of olfactory sensory neurons. Neuron. 2005; 48:1039–1053. [PubMed: 16364906]

Mercado J, Gordon-Shaag A, Zagotta WN, Gordon SE. Ca2+-dependent desensitization of TRPV2 channels is mediated by hydrolysis of phosphatidylinositol 4,5-bisphosphate. J Neurosci. 2010; 30:13338–13347. [PubMed: 20926660]

Merksamer PI, Trusina A, Papa FR. Real-time redox measurements during endoplasmic reticulum stress reveal interlinked protein folding functions. Cell. 2008; 135:933–947. [PubMed: 19026441]

Metzger F, Repunte-Canonigo V, Matsushita S, Akemann W, Diez-Garcia J, Ho CS, Iwasato T, Grandes P, Itohara S, Joho RH, Knopfel T. Transgenic mice expressing a pH and Cl- sensing yellow-fluorescent protein under the control of a potassium channel promoter. Eur J Neurosci. 2002; 15:40–50. [PubMed: 11860505]

Meyer AJ, Dick TP. Fluorescent protein-based redox probes. Antioxid Redox Signal. 2010; 13:621–650. [PubMed: 20088706]

Micheva KD, Holz RW, Smith SJ. Regulation of presynaptic phosphatidylinositol 4,5-biphosphate by neuronal activity. J Cell Biol. 2001; 154:355–368. [PubMed: 11470824]

Miesenbock G, De Angelis DA, Rothman JE. Visualizing secretion and synaptic transmission with pH-sensitive green fluorescent proteins. Nature. 1998; 394:192–195. [PubMed: 9671304]

Miyawaki A, Llopis J, Heim R, McCaffery JM, Adams JA, Ikura M, Tsien RY. Fluorescent indicators for Ca2+ based on green fluorescent proteins and calmodulin. Nature. 1997; 388:882–887. [PubMed: 9278050]

Mochizuki N, Yamashita S, Kurokawa K, Ohba Y, Nagai T, Miyawaki A, Matsuda M. Spatio-temporal images of growth-factor-induced activation of Ras and Rap1. Nature. 2001; 411:1065–1068. [PubMed: 11429608]

Mukhtarov M, Markova O, Real E, Jacob Y, Buldakova S, Bregestovski P. Monitoring of chloride and activity of glycine receptor channels using genetically encoded fluorescent sensors. Philos Transact A Math Phys Eng Sci. 2008; 366:3445–3462. [PubMed: 18632458]

Muller FL. A critical evaluation of cpYFP as a probe for superoxide. Free Radic Biol Med. 2009; 47:1779–1780. [PubMed: 19778603]

Murakoshi H, Lee SJ, Yasuda R. Highly sensitive and quantitative FRET-FLIM imaging in single dendritic spines using improved non-radiative YFP. Brain Cell Biol. 2008; 36:31–42. [PubMed: 18512154]

Nagai T, Sawano A, Park ES, Miyawaki A. Circularly permuted green fluorescent proteins engineered to sense Ca2+ Proc Natl Acad Sci USA. 2001; 98:3197–3202. [PubMed: 11248055]

Nagai T, Yamada S, Tominaga T, Ichikawa M, Miyawaki A. Expanded dynamic range of fluorescent indicators for Ca(2+) by circularly permuted yellow fluorescent proteins. Proc Natl Acad Sci USA. 2004; 101:10554–10559. [PubMed: 15247428]

Nagai Y, Miyazaki M, Aoki R, Zama T, Inouye S, Hirose K, Iino M, Hagiwara M. A fluorescent indicator for visualizing cAMP-induced phosphorylation in vivo. Nat Biotechnol. 2000; 18:313–316. [PubMed: 10700148]

Nakai J, Ohkura M, Imoto K. A high signal-to-noise Ca(2+) probe composed of a single green fluorescent protein. Nat Biotechnol. 2001; 19:137–141. [PubMed: 11175727]

Nakamura T, Aoki K, Matsuda M. FRET imaging and in silico simulation: analysis of the signaling network of nerve growth factor-induced neuritogenesis. Brain Cell Biol. 2008; 36:19–30. [PubMed: 18654855]

Nausch LW, Ledoux J, Bonev AD, Nelson MT, Dostmann WR. Differential patterning of cGMP in vascular smooth muscle cells revealed by single GFP-linked biosensors. Proc Natl Acad Sci USA. 2008; 105:365–370. [PubMed: 18165313]

Nelson CP, Nahorski SR, Challiss RA. Temporal profiling of changes in phosphatidylinositol 4,5-bisphosphate, inositol 1,4,5-trisphosphate and diacylglycerol allows comprehensive analysis of phospholipase C-initiated signalling in single neurons. J Neurochem. 2008; 107:602–615. [PubMed: 18665913]

Nemani VM, Lu W, Berge V, Nakamura K, Onoa B, Lee MK, Chaudhry FA, Nicoll RA, Edwards RH. Increased expression of alpha-synuclein reduces neurotransmitter release by inhibiting synaptic vesicle reclustering after endocytosis. Neuron. 2010; 65:66–79. [PubMed: 20152114]

Newman RH, Fosbrink MD, Zhang J. Genetically Encodable Fluorescent Biosensors for Tracking Signaling Dynamics in Living Cells. Chem Rev. 2011; 111:3614–3666. [PubMed: 21456512]

Nikolaev VO, Bunemann M, Hein L, Hannawacker A, Lohse MJ. Novel single chain cAMP sensors for receptor-induced signal propagation. J Biol Chem. 2004; 279:37215–37218. [PubMed: 15231839]

Nishioka T, Aoki K, Hikake K, Yoshizaki H, Kiyokawa E, Matsuda M. Rapid turnover rate of phosphoinositides at the front of migrating MDCK cells. Mol Biol Cell. 2008; 19:4213–4223. [PubMed: 18685081]

Nobles M, Benians A, Tinker A. Heterotrimeric G proteins precouple with G protein-coupled receptors in living cells. Proc Natl Acad Sci USA. 2005; 102:18706–18711. [PubMed: 16352729]

Oancea E, Teruel MN, Quest AF, Meyer T. Green fluorescent protein (GFP)-tagged cysteine-rich domains from protein kinase C as fluorescent indicators for diacylglycerol signaling in living cells. J Cell Biol. 1998; 140:485–498. [PubMed: 9456311]

Okubo Y, Kakizawa S, Hirose K, Iino M. Visualization of IP(3) dynamics reveals a novel AMPA receptor-triggered IP(3) production pathway mediated by voltage-dependent Ca(2+) influx in Purkinje cells. Neuron. 2001; 32:113–122. [PubMed: 11604143]

Okumoto S, Looger LL, Micheva KD, Reimer RJ, Smith SJ, Frommer WB. Detection of glutamate release from neurons by genetically encoded surface-displayed FRET nanosensors. Proc Natl Acad Sci USA. 2005; 102:8740–8745. [PubMed: 15939876]

Okumoto S, Takanaga H, Frommer WB. Quantitative imaging for discovery and assembly of the metabo-regulome. New Phytol. 2008; 180:271–295. [PubMed: 19138219]

Ostergaard H, Henriksen A, Hansen FG, Winther JR. Shedding light on disulfide bond formation: engineering a redox switch in green fluorescent protein. EMBO J. 2001; 20:5853–5862. [PubMed: 11689426]

Pacary E, Heng J, Azzarelli R, Riou P, Castro D, Lebel-Potter M, Parras C, Bell DM, Ridley AJ, Parsons M, Guillemot F. Proneural transcription factors regulate different steps of cortical neuron migration through Rnd-mediated inhibition of RhoA signaling. Neuron. 2011; 69:1069–1084. [PubMed: 21435554]

Palmer AE, Giacomello M, Kortemme T, Hires SA, Lev-Ram V, Baker D, Tsien RY. Ca2+ indicators based on computationally redesigned calmodulin-peptide pairs. Chem Biol. 2006; 13:521–530. [PubMed: 16720273]

Patterson GH, Piston DW, Barisas BG. Forster distances between green fluorescent protein pairs. Anal Biochem. 2000; 284:438–440. [PubMed: 10964438]

Pertz O, Hodgson L, Klemke RL, Hahn KM. Spatiotemporal dynamics of RhoA activity in migrating cells. Nature. 2006; 440:1069–1072. [PubMed: 16547516]

Poburko D, Santo-Domingo J, Demaurex N. Dynamic Regulation of the Mitochondrial Proton Gradient during Cytosolic Calcium Elevations. J Biol Chem. 2011; 286:11672–11684. [PubMed: 21224385]

Pond BB, Berglund K, Kuner T, Feng G, Augustine GJ, Schwartz-Bloom RD. The chloride transporter Na(+)-K(+)-Cl- cotransporter isoform-1 contributes to intracellular chloride increases after in vitro ischemia. J Neurosci. 2006; 26:1396–1406. [PubMed: 16452663]

Prebil M, Chowdhury HH, Zorec R, Kreft M. Changes in cytosolic glucose level in ATP stimulated live astrocytes. Biochem Biophys Res Commun. 2011a; 405:308–313. [PubMed: 21237134]

Prebil M, Vardjan N, Jensen J, Zorec R, Kreft M. Dynamic monitoring of cytosolic glucose in single astrocytes. Glia. 2011b; 59:903–913. [PubMed: 21381116]

Qin Y, Dittmer PJ, Park JG, Jansen KB, Palmer AE. Measuring steady-state and dynamic endoplasmic reticulum and Golgi Zn2+ with genetically encoded sensors. Proc Natl Acad Sci USA. 2011; 108:7351–7356. [PubMed: 21502528]

Quinn KV, Behe P, Tinker A. Monitoring changes in membrane phosphatidylinositol 4,5-bisphosphate in living cells using a domain from the transcription factor tubby. J Physiol. 2008; 586:2855–2871. [PubMed: 18420701]

Remus TP, Zima AV, Bossuyt J, Bare DJ, Martin JL, Blatter LA, Bers DM, Mignery GA. Biosensors to measure inositol 1,4,5-trisphosphate concentration in living cells with spatiotemporal resolution. J Biol Chem. 2006; 281:608–616. [PubMed: 16249182]

Rochais F, Vilardaga JP, Nikolaev VO, Bunemann M, Lohse MJ, Engelhardt S. Real-time optical recording of beta1-adrenergic receptor activation reveals supersensitivity of the Arg389 variant to carvedilol. J Clin Invest. 2007; 117:229–235. [PubMed: 17200720]

Romoser VA, Hinkle PM, Persechini A. Detection in living cells of Ca2+-dependent changes in the fluorescence emission of an indicator composed of two green fluorescent protein variants linked by a calmodulin-binding sequence. A new class of fluorescent indicators. J Biol Chem. 1997; 272:13270–13274. [PubMed: 9148946]

Ryan TA. Presynaptic imaging techniques. Curr Opin Neurobiol. 2001; 11:544–549. [PubMed: 11595486]

Sabouri-Ghomi M, Wu Y, Hahn K, Danuser G. Visualizing and quantifying adhesive signals. Curr Opin Cell Biol. 2008; 20:541–550. [PubMed: 18586481]

Saneyoshi T, Wayman G, Fortin D, Davare M, Hoshi N, Nozaki N, Natsume T, Soderling TR. Activity-dependent synaptogenesis: regulation by a CaM-kinase kinase/CaM-kinase I/betaPIX signaling complex. Neuron. 2008; 57:94–107. [PubMed: 18184567]

Sankaranarayanan S, De Angelis D, Rothman JE, Ryan TA. The use of pHluorins for optical measurements of presynaptic activity. Biophys J. 2000; 79:2199–2208. [PubMed: 11023924]

Sankaranarayanan S, Ryan TA. Calcium accelerates endocytosis of vSNAREs at hippocampal synapses. Nat Neurosci. 2001; 4:129–136. [PubMed: 11175872]

Santagata S, Boggon TJ, Baird CL, Gomez CA, Zhao J, Shan WS, Myszka DG, Shapiro L. G-protein signaling through tubby proteins. Science. 2001; 292:2041–2050. [PubMed: 11375483]

Sasaki K, Sato M, Umezawa Y. Fluorescent indicators for Akt/protein kinase B and dynamics of Akt activity visualized in living cells. J Biol Chem. 2003; 278:30945–30951. [PubMed: 12773546]

Sato M, Nakajima T, Goto M, Umezawa Y. Cell-based indicator to visualize picomolar dynamics of nitric oxide release from living cells. Anal Chem. 2006; 78:8175–8182. [PubMed: 17165805]

Sato M, Ueda Y, Shibuya M, Umezawa Y. Locating inositol 1,4,5-trisphosphate in the nucleus and neuronal dendrites with genetically encoded fluorescent indicators. Anal Chem. 2005; 77:4751–4758. [PubMed: 16053285]

Schwarzlander M, Logan DC, Fricker MD, Sweetlove L. The circularly permuted yellow fluorescent protein cpYFP that has been used as a superoxide probe is highly responsive to pH but not superoxide in mitochondria: implications for the existence of superoxide ‘flashes’. Biochem J. 2011

Shafer OT, Kim DJ, Dunbar-Yaffe R, Nikolaev VO, Lohse MJ, Taghert PH. Widespread receptivity to neuropeptide PDF throughout the neuronal circadian clock network of Drosophila revealed by real-time cyclic AMP imaging. Neuron. 2008; 58:223–237. [PubMed: 18439407]

Shang Y, Claridge-Chang A, Sjulson L, Pypaert M, Miesenbock G. Excitatory local circuits and their implications for olfactory processing in the fly antennal lobe. Cell. 2007; 128:601–612. [PubMed: 17289577]

Slemmer JE, Matsushita S, De Zeeuw CI, Weber JT, Knopfel T. Glutamate-induced elevations in intracellular chloride concentration in hippocampal cell cultures derived from EYFP-expressing mice. Eur J Neurosci. 2004; 19:2915–2922. [PubMed: 15182298]

Srivastava J, Barber DL, Jacobson MP. Intracellular pH sensors: design principles and functional significance. Physiology (Bethesda). 2007; 22:30–39. [PubMed: 17289928]

Stauffer TP, Ahn S, Meyer T. Receptor-induced transient reduction in plasma membrane PtdIns(4,5)P2 concentration monitored in living cells. Curr Biol. 1998; 8:343–346. [PubMed: 9512420]

Suh BC, Horowitz LF, Hirdes W, Mackie K, Hille B. Regulation of KCNQ2/KCNQ3 current by G protein cycling: the kinetics of receptor-mediated signaling by Gq. J Gen Physiol. 2004; 123:663–683. [PubMed: 15173220]

Svoboda K, Yasuda R. Principles of two-photon excitation microscopy and its applications to neuroscience. Neuron. 2006; 50:823–839. [PubMed: 16772166]

Szentpetery Z, Balla A, Kim YJ, Lemmon MA, Balla T. Live cell imaging with protein domains capable of recognizing phosphatidylinositol 4,5-bisphosphate; a comparative study. BMC Cell Biol. 2009; 10:67. [PubMed: 19769794]

Takanaga H, Chaudhuri B, Frommer WB. GLUT1 and GLUT9 as major contributors to glucose influx in HepG2 cells identified by a high sensitivity intramolecular FRET glucose sensor. Biochim Biophys Acta. 2008; 1778:1091–1099. [PubMed: 18177733]

Tani H, Dulla CG, Huguenard JR, Reimer RJ. Glutamine is required for persistent epileptiform activity in the disinhibited neocortical brain slice. J Neurosci. 2010; 30:1288–1300. [PubMed: 20107056]

Tanimura A, Nezu A, Morita T, Turner RJ, Tojyo Y. Fluorescent biosensor for quantitative real-time measurements of inositol 1,4,5-trisphosphate in single living cells. J Biol Chem. 2004; 279:38095–38098. [PubMed: 15272011]

Tateyama M, Abe H, Nakata H, Saito O, Kubo Y. Ligand-induced rearrangement of the dimeric metabotropic glutamate receptor 1alpha. Nat Struct Mol Biol. 2004; 11:637–642. [PubMed: 15184890]

Thorsen TS, Madsen KL, Rebola N, Rathje M, Anggono V, Bach A, Moreira IS, Stuhr-Hansen N, Dyhring T, Peters D, Beuming T, Huganir R, Weinstein H, Mulle C, Stromgaard K, Ronn LC, Gether U. Identification of a small-molecule inhibitor of the PICK1 PDZ domain that inhibits hippocampal LTP and LTD. Proc Natl Acad Sci USA. 2010; 107:413–418. [PubMed: 20018661]

Tsien RY. The green fluorescent protein. Annu Rev Biochem. 1998; 67:509–544. [PubMed: 9759496]

Tsou P, Zheng B, Hsu CH, Sasaki AT, Cantley LC. A Fluorescent Reporter of AMPK Activity and Cellular Energy Stress. Cell Metab. 2011; 13:476–486. [PubMed: 21459332]

Tuffy LP, Concannon CG, D'Orsi B, King MA, Woods I, Huber HJ, Ward MW, Prehn JH. Characterization of Puma-dependent and Puma-independent neuronal cell death pathways following prolonged proteasomal inhibition. Mol Cell Biol. 2010; 30:5484–5501. [PubMed: 20921277]

van der Wal J, Habets R, Varnai P, Balla T, Jalink K. Monitoring agonist-induced phospholipase C activation in live cells by fluorescence resonance energy transfer. J Biol Chem. 2001; 276:15337–15344. [PubMed: 11152673]

Vanderklish PW, Krushel LA, Holst BH, Gally JA, Crossin KL, Edelman GM. Marking synaptic activity in dendritic spines with a calpain substrate exhibiting fluorescence resonance energy transfer. Proc Natl Acad Sci USA. 2000; 97:2253–2258. [PubMed: 10688895]

Varnai P, Balla T. Visualization of phosphoinositides that bind pleckstrin homology domains: calcium- and agonist-induced dynamic changes and relationship to myo-[3H]inositol-labeled phosphoinositide pools. J Cell Biol. 1998; 143:501–510. [PubMed: 9786958]

Varnai P, Balla T. Live cell imaging of phosphoinositide dynamics with fluorescent protein domains. Biochim Biophys Acta. 2006; 1761:957–967. [PubMed: 16702024]

Vesce S, Jekabsons MB, Johnson-Cadwell LI, Nicholls DG. Acute glutathione depletion restricts mitochondrial ATP export in cerebellar granule neurons. J Biol Chem. 2005; 280:38720–38728. [PubMed: 16172117]

Vilardaga JP, Bunemann M, Krasel C, Castro M, Lohse MJ. Measurement of the millisecond activation switch of G protein-coupled receptors in living cells. Nat Biotechnol. 2003; 21:807–812. [PubMed: 12808462]

Vincent P, Gervasi N, Zhang J. Real-time monitoring of cyclic nucleotide signaling in neurons using genetically encoded FRET probes. Brain Cell Biol. 2008; 36:3–17. [PubMed: 18941898]

Vinkenborg JL, Koay MS, Merkx M. Fluorescent imaging of transition metal homeostasis using genetically encoded sensors. Curr Opin Chem Biol. 2010; 14:231–237. [PubMed: 20036601]

Violin JD, Zhang J, Tsien RY, Newton AC. A genetically encoded fluorescent reporter reveals oscillatory phosphorylation by protein kinase C. J Cell Biol. 2003; 161:899–909. [PubMed: 12782683]

Wachter RM, Elsliger MA, Kallio K, Hanson GT, Remington SJ. Structural basis of spectral shifts in the yellow-emission variants of green fluorescent protein. Structure. 1998; 6:1267–1277. [PubMed: 9782051]

Wachter RM, Yarbrough D, Kallio K, Remington SJ. Crystallographic and energetic analysis of binding of selected anions to the yellow variants of green fluorescent protein. J Mol Biol. 2000; 301:157–171. [PubMed: 10926499]

Wang Q, Shui B, Kotlikoff MI, Sondermann H. Structural basis for calcium sensing by GCaMP2. Structure. 2008a; 16:1817–1827. [PubMed: 19081058]

Wang W, Fang H, Groom L, Cheng A, Zhang W, Liu J, Wang X, Li K, Han P, Zheng M, Yin J, Wang W, Mattson MP, Kao JP, Lakatta EG, Sheu SS, Ouyang K, Chen J, Dirksen RT, Cheng H. Superoxide flashes in single mitochondria. Cell. 2008b; 134:279–290. [PubMed: 18662543]

Ward MW, Rehm M, Duessmann H, Kacmar S, Concannon CG, Prehn JH. Real time single cell analysis of Bid cleavage and Bid translocation during caspase-dependent and neuronal caspase-independent apoptosis. J Biol Chem. 2006; 281:5837–5844. [PubMed: 16407197]

Wardman P. Fluorescent and luminescent probes for measurement of oxidative and nitrosative species in cells and tissues: progress, pitfalls, and prospects. Free Radic Biol Med. 2007; 43:995–1022. [PubMed: 17761297]

Waseem T, Mukhtarov M, Buldakova S, Medina I, Bregestovski P. Genetically encoded Cl-Sensor as a tool for monitoring of Cl-dependent processes in small neuronal compartments. J Neurosci Methods. 2010; 193:14–23. [PubMed: 20705097]

Willemse M, Janssen E, de Lange F, Wieringa B, Fransen J. ATP and FRET--a cautionary note. Nat Biotechnol. 2007; 25:170–172. [PubMed: 17287746]

Willets JM, Nelson CP, Nahorski SR, Challiss RA. The regulation of M1 muscarinic acetylcholine receptor desensitization by synaptic activity in cultured hippocampal neurons. J Neurochem. 2007; 103:2268–2280. [PubMed: 17908240]

Willoughby D, Cooper DM. Live-cell imaging of cAMP dynamics. Nat Methods. 2008; 5:29–36. [PubMed: 18165805]

Winterbourn CC. Reconciling the chemistry and biology of reactive oxygen species. Nat Chem Biol. 2008; 4:278–286. [PubMed: 18421291]

Xu C, Watras J, Loew LM. Kinetic analysis of receptor-activated phosphoinositide turnover. J Cell Biol. 2003; 161:779–791. [PubMed: 12771127]

Xu X, Gerard AL, Huang BC, Anderson DC, Payan DG, Luo Y. Detection of programmed cell death using fluorescence energy transfer. Nucleic Acids Res. 1998; 26:2034–2035. [PubMed: 9518501]

Yan HD, Villalobos C, Andrade R. TRPC Channels Mediate a Muscarinic Receptor-Induced Afterdepolarization in Cerebral Cortex. J Neurosci. 2009; 29:10038–10046. [PubMed: 19675237]

Yoshizaki H, Ohba Y, Kurokawa K, Itoh RE, Nakamura T, Mochizuki N, Nagashima K, Matsuda M. Activity of Rho-family GTPases during cell division as visualized with FRET-based probes. J Cell Biol. 2003; 162:223–232. [PubMed: 12860967]

Yu D, Ponomarev A, Davis RL. Altered representation of the spatial code for odors after olfactory classical conditioning; memory trace formation by synaptic recruitment. Neuron. 2004; 42:437–449. [PubMed: 15134640]

Zaccolo M, De Giorgi F, Cho CY, Feng L, Knapp T, Negulescu PA, Taylor SS, Tsien RY, Pozzan T. A genetically encoded, fluorescent indicator for cyclic AMP in living cells. Nat Cell Biol. 2000; 2:25–29. [PubMed: 10620803]

Zadran S, Jourdi H, Rostamiani K, Qin Q, Bi X, Baudry M. Brain-derived neurotrophic factor and epidermal growth factor activate neuronal m-calpain via mitogen-activated protein kinase-dependent phosphorylation. J Neurosci. 2010; 30:1086–1095. [PubMed: 20089917]

Zhang H, Macara IG. The PAR-6 polarity protein regulates dendritic spine morphogenesis through p190 RhoGAP and the Rho GTPase. Dev Cell. 2008; 14:216–226. [PubMed: 18267090]

Zhang J, Ma Y, Taylor SS, Tsien RY. Genetically encoded reporters of protein kinase A activity reveal impact of substrate tethering. Proc Natl Acad Sci USA. 2001; 98:14997–15002. [PubMed: 11752448]

Zhang J, Wang Y, Chi Z, Keuss MJ, Pai YM, Kang HC, Shin JH, Bugayenko A, Wang H, Xiong Y, Pletnikov MV, Mattson MP, Dawson TM, Dawson VL. The AAA(+) ATPase Thorase Regulates AMPA Receptor-Dependent Synaptic Plasticity and Behavior. Cell. 2011; 145:284–299. [PubMed: 21496646]

Zhang Q, Li Y, Tsien RW. The dynamic control of kiss-and-run and vesicular reuse probed with single nanoparticles. Science. 2009; 323:1448–1453. [PubMed: 19213879]

Zuo Y, Lubischer JL, Kang H, Tian L, Mikesh M, Marks A, Scofield VL, Maika S, Newman C, Krieg P, Thompson WJ. Fluorescent proteins expressed in mouse transgenic lines mark subsets of glia, neurons, macrophages, and dendritic cells for vital examination. J Neurosci. 2004; 24:10999–11009. [PubMed: 15590915]

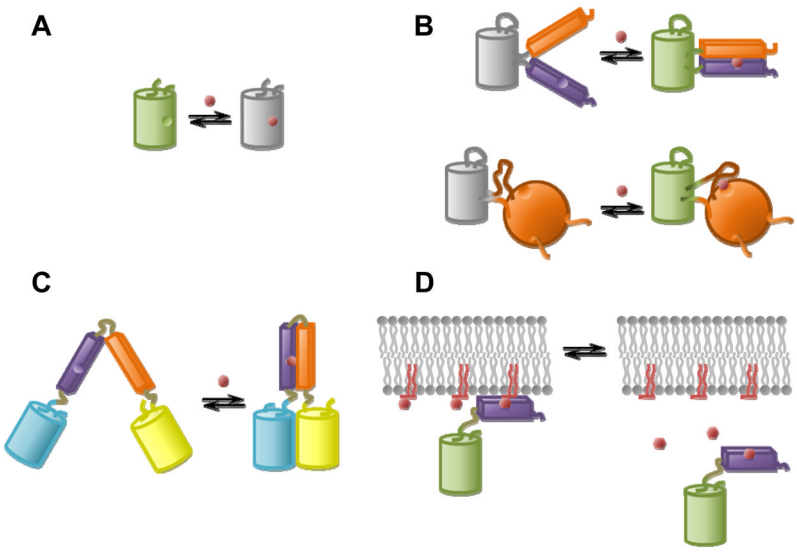

Figure 1.

Design strategies for engineering genetically-encoded indicators. Fluorescent proteins are shown as cylinders. Sensor domains are boxes or spheres in orange or purple. Target ligands are shown in red. Examples are shown for indicators of small molecule analytes, but the designs can also be applied to engineer indicators of enzyme activity or protein activation. (A) A single environmentally-sensitive fluorescent protein acts as the sensor and reporter. (B) Circular-permutation of a fluorescent protein renders its fluorescence sensitive to a conformational change in a sensor domain. The sensor domain may consist of two proteins or peptides attached to the new termini of the circularly-permuted fluorescent protein (top). Alternatively, the circularly-permuted fluorescent protein may be inserted into a sensor protein in a region that experiences a conformation change (bottom). (C) Fluorescent proteins are attached to two parts of a sensor domain that experience a relative motion, and the conformational change can alter the distance or orientation between the fluorescent proteins, changing the FRET efficiency. (D) A fluorescent protein is attached to a sensor domain that localizes differently depending on ligand binding or activation. In the example shown, the indicator localizes to the plasma membrane or cytosol depending on the ligand status.

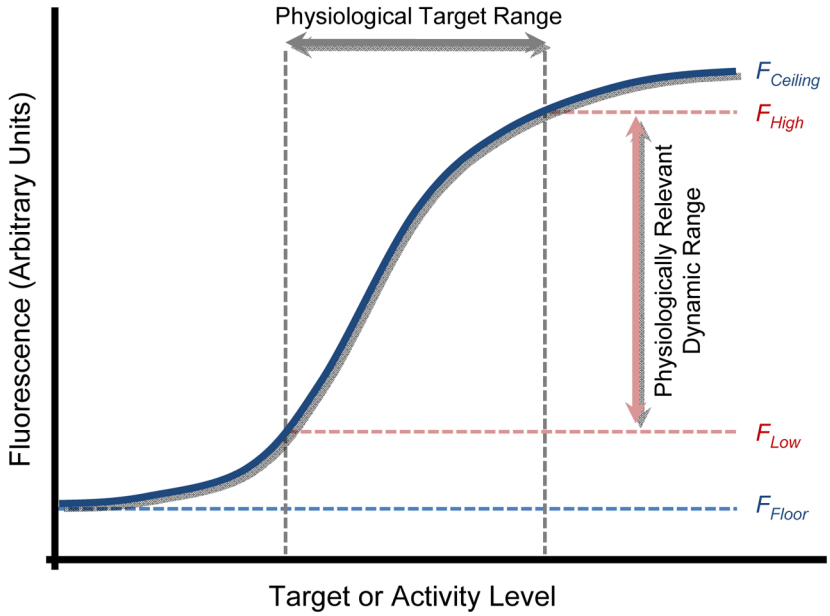

Figure 2.

A hypothetical GEI dose-response curve. The physiologically relevant dynamic range (F_{High}/F_{Low}) is usually smaller than the GEI's maximum fluorescence dynamic range ($F_{Ceiling}/F_{Floor}$) because only a portion of the total sensing range is sampled in the physiological scenario.

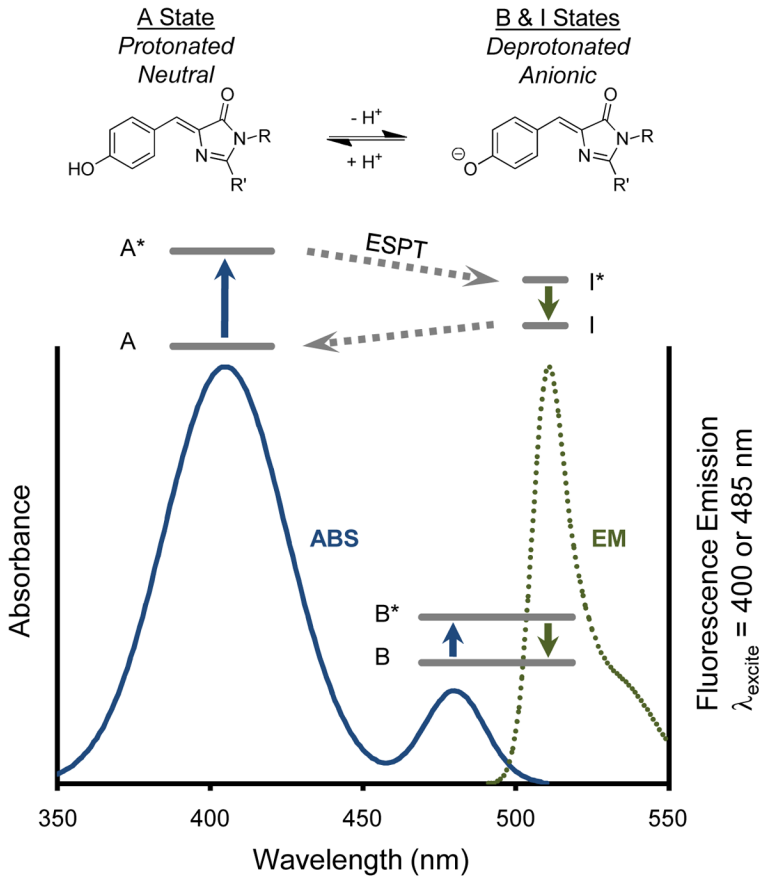

Figure 3.

Protonation of the fluorescent protein chromophore and its effects on the absorbance and fluorescence spectra. The example is theoretical but based on the wild type green fluorescent protein chromophore and spectra. In the physiological pH range, the chromophore can be protonated in a neutral “A” state or ionized in an anionic “B” state (top). Two peaks in the absorbance spectrum (solid blue curve) reflect the two states. A single peak is observed in the fluorescence emission spectrum (dotted green curve) when exciting the B state, and a similar emission spectrum is observed when exciting the A state because excited-state proton transfer occurs, creating an anionic excited state I* very similar to the B* anionic excited state. Simplified Jablonski diagrams are superimposed to represent energy transitions following absorption (blue arrow) and resulting in fluorescence emission (green arrow). The B and B* energy levels are shown lower in the diagram for visual clarity and are not indicative of actual energy differences with the A or I states.